Figure 8.2 A plot of driving force ΔG_m versus reaction onset temperature for transformation to acicular ferrite (large prior austenite grains) and to bainite (small prior austenite grains). For comparison purposes, the relationship between ΔG_m and T_H derived from the data of Steven & Haynes (1956) is included, indicating that the welding alloys considered require a somewhat lower driving force for nucleation.
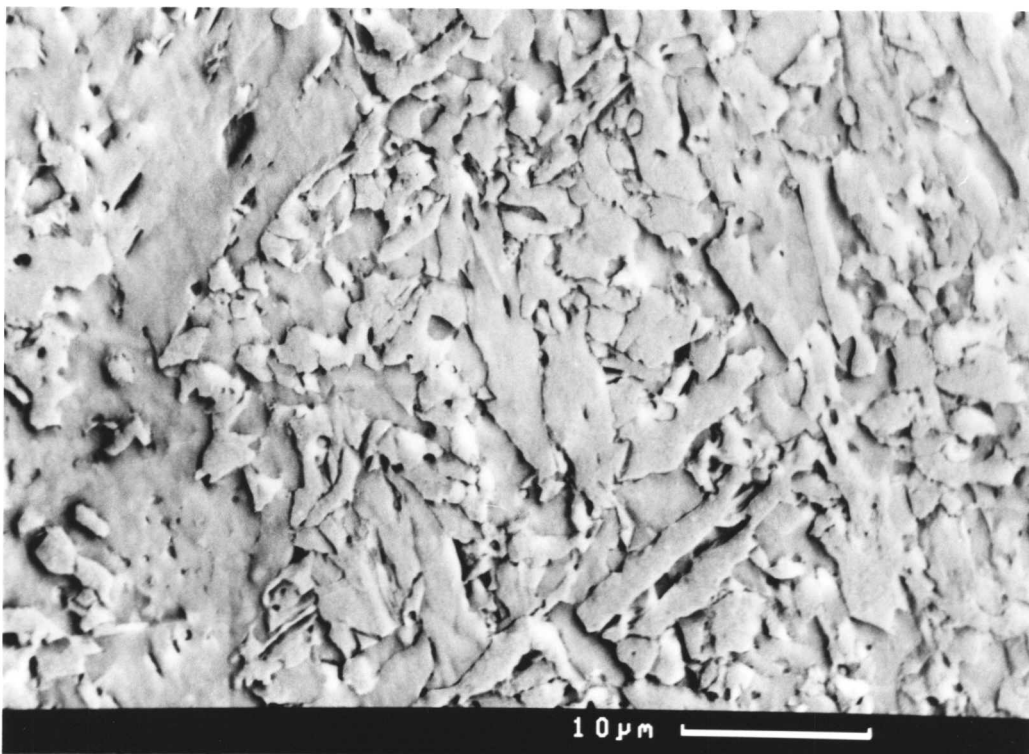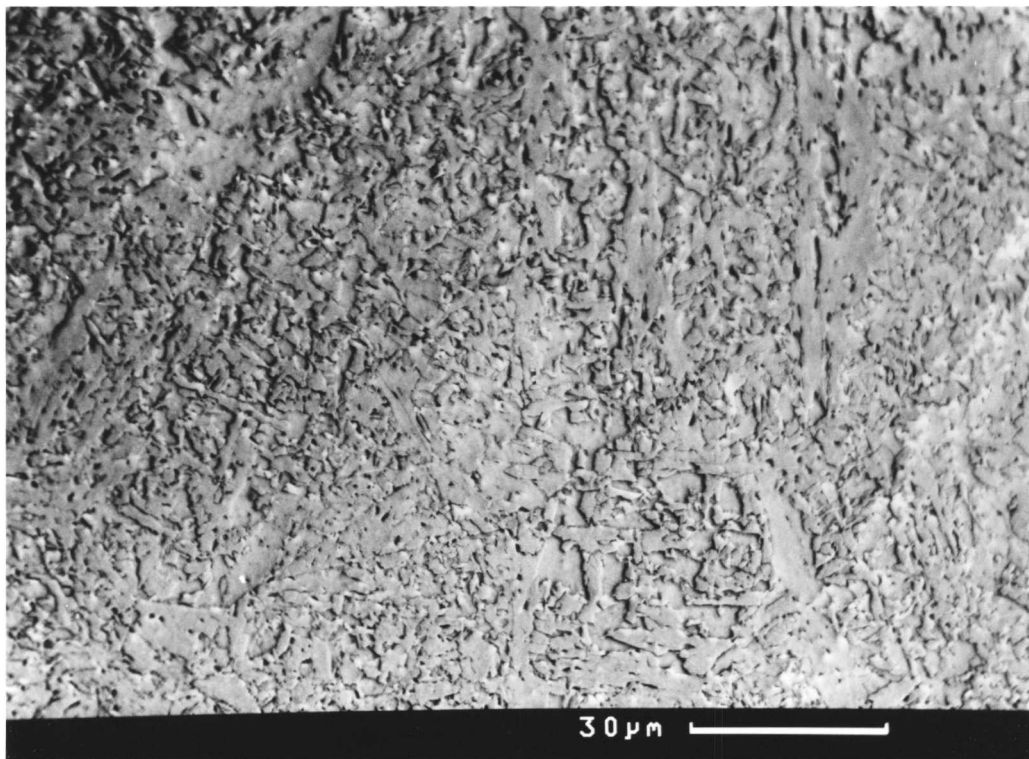
Figure 8.3 The microstructure of alloy 116, austenitised for 10 min. at 1375°C, cooled at $5°Cs^{-1}$. a) low magnification image b) high magnification image showing the acicular ferrite structure.
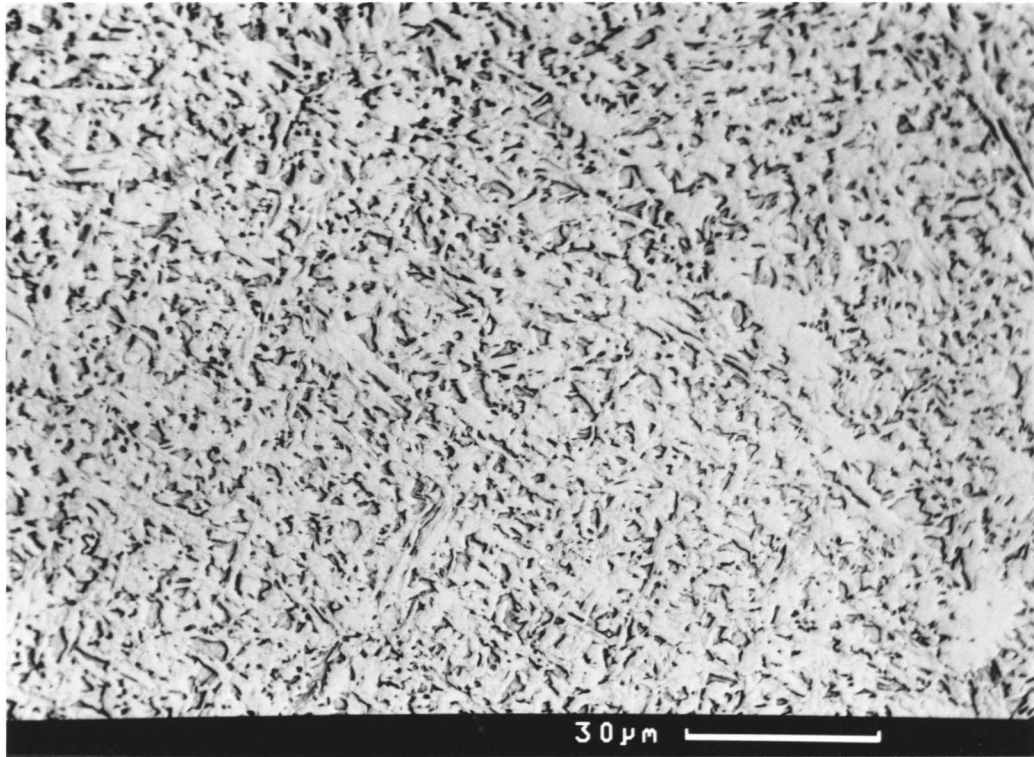
Figure 8.4 The microstructure of alloy 116, austenitised for 3 min. at 1350°C, cooled at $0.5°Cs^{-1}$. The transformation was interrupted by quenching at 450°C.
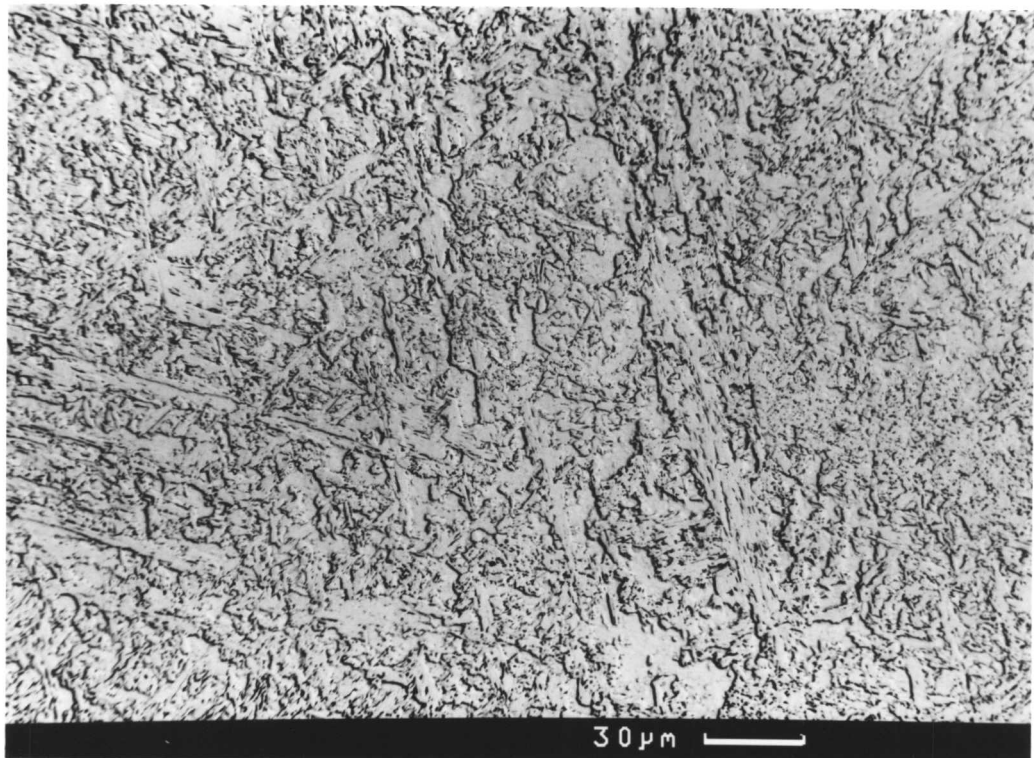
Figure 8.5 The microstructure of alloy 115, austenitised for 10 min at 1375°C, cooled at $5°Cs^{-1}$.

144
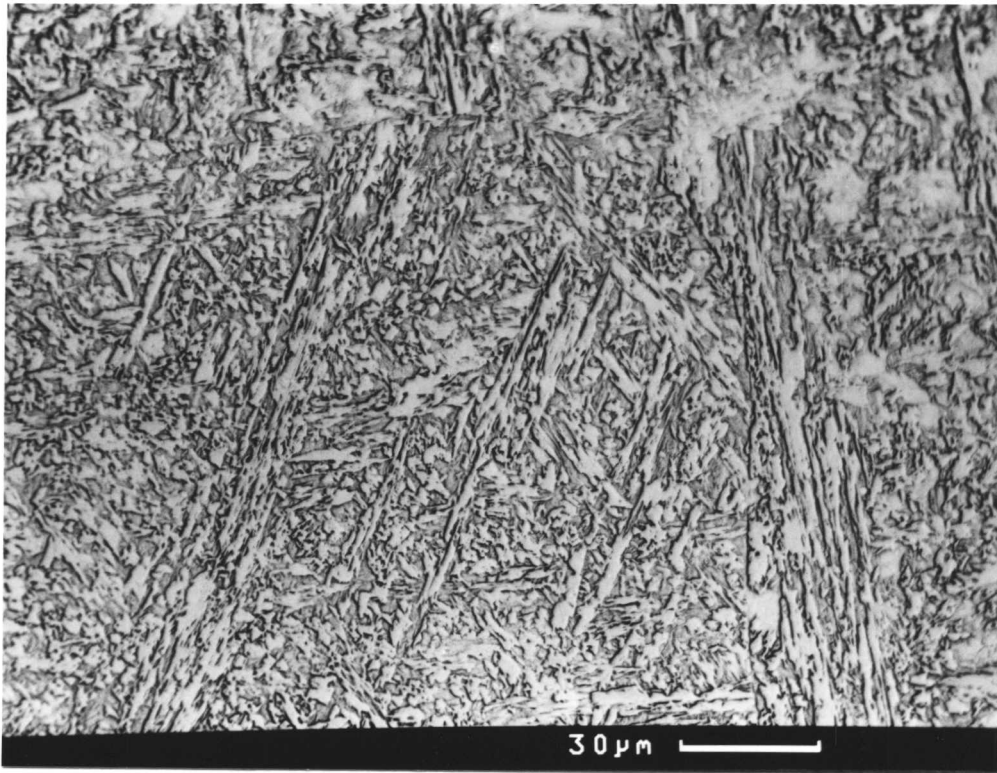
Figure 8.6 The microstructure of alloy 115, austenitised for 3 min at 1350°C, cooled at $0.05°Cs^{-1}$. The transformation was interrupted by quenching at 400°C.
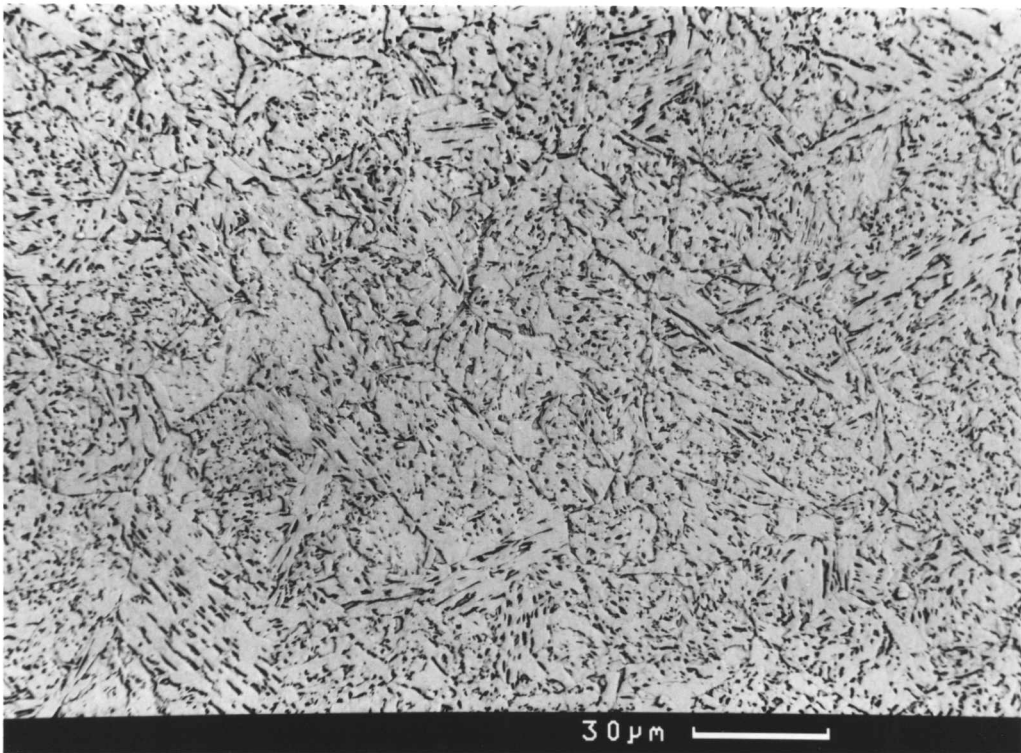
Figure 8.7 The microstructure of alloy 116, austenitised for 5 min at 1000°C, cooled at $5°Cs^{-1}$.
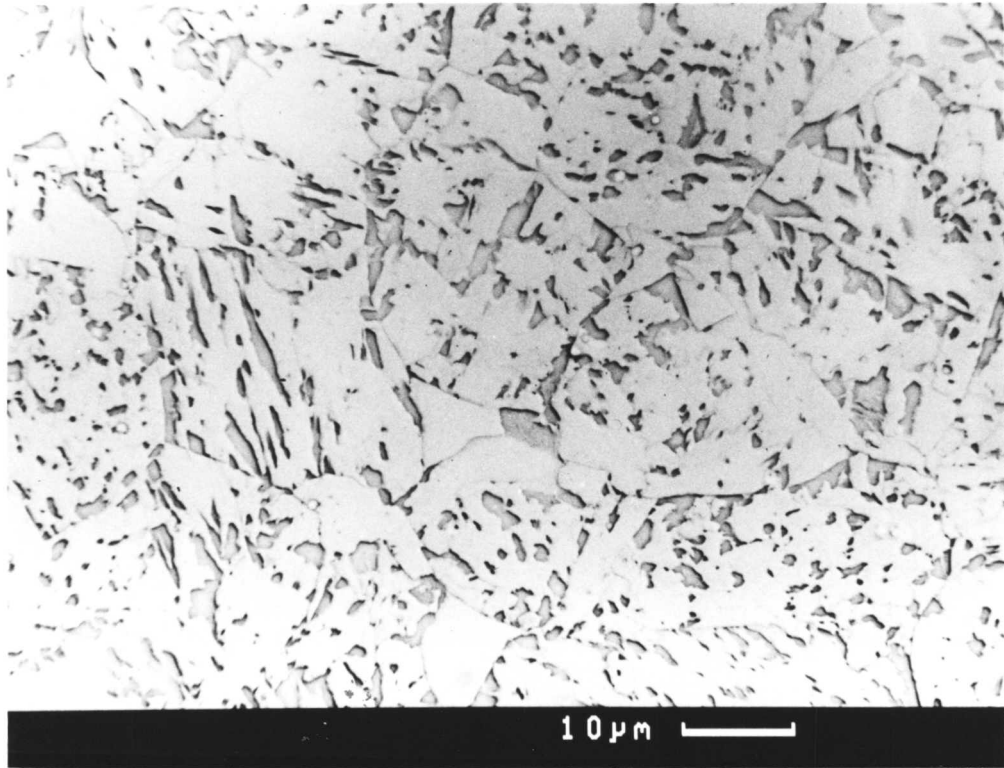
Figure 8.8 The microstructure of alloy 116, austenitised for 5 min at 1000°C, cooled at $0.5°Cs^{-1}$.
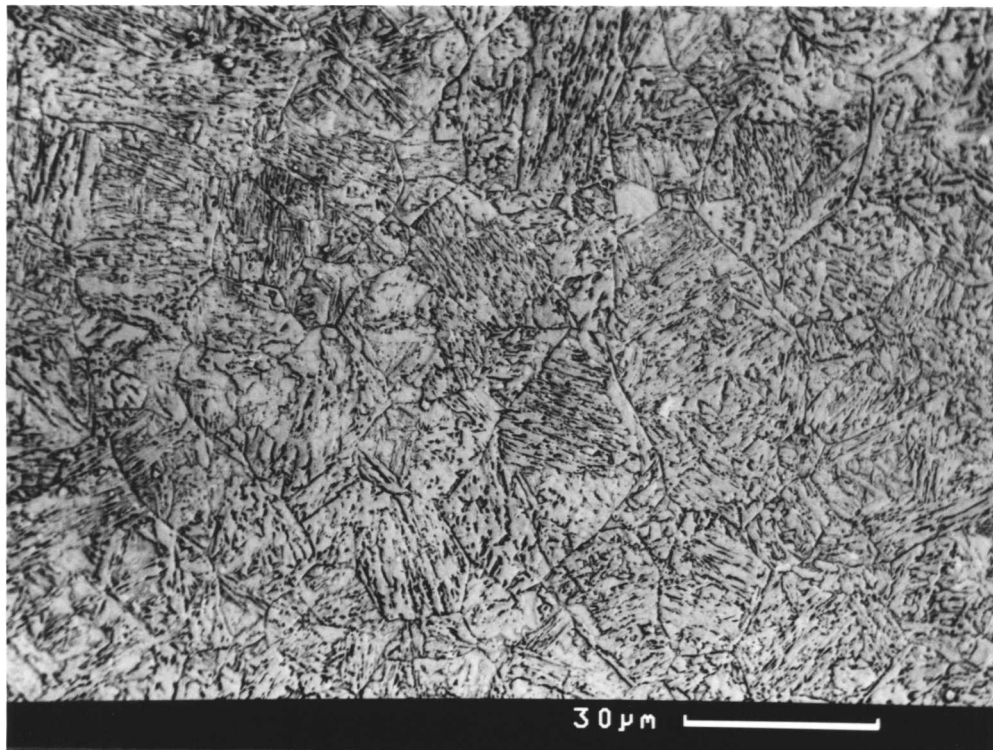
Figure 8.9 The microstructure of alloy 115, austenitised for 5 min at 1000°C, cooled at $5°Cs^{-1}$.

146

Figure 8.10 The microstructure of alloy 115, austenitised for 5 min at 1000°C, cooled at $0.05°Cs^{-1}$.

Low Carbon Steel data from Steven & Haynes (1956)

$G_N = 3.12\ T_H - 2148\ \mathrm{J\ mol}^{-1}$

$G_N = 3.515\ T_H - 2420\ \mathrm{J\ mol}^{-1}$

$G_N = 3.636\ T_H - 2540\ \mathrm{J\ mol}^{-1}$

Figure 8.11 A plot of the driving force at the highest temperature at which displacive transformations are observed in the lowest carbon steels considered by Steven & Haynes (1956). Also included are the best fit lines representing the driving force at B_S for the welding alloys, and the overall relationship from the data of Steven & Haynes.

CHAPTER 9

Microstructure and Properties of Isothermally Transformed High Strength Weld Metals

9.1 Introduction

The aim of work presented in this chapter was to consolidate and apply the results presented in the earlier chapters of the thesis. Thus, the kinetics of acicular ferrite formation were investigated as a function of alloy chemistry and isothermal transformation temperature. At the same time an attempt was made to rationalise the morphology and strength of the resulting mixed acicular ferrite and martensite microstructures. The data were also interpreted in terms of the thermodynamics and mechanism of acicular ferrite reaction.

Homogenised samples of reaustenitised weld metals were isothermally transformed to investigate the following:
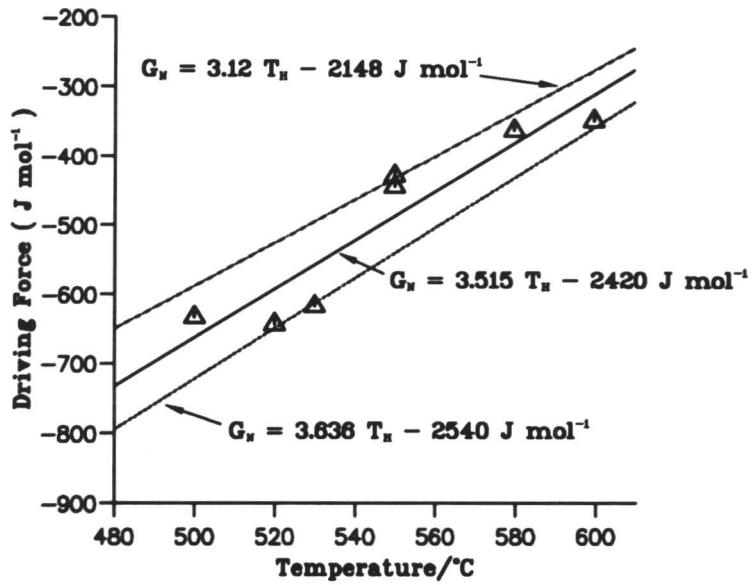
(a) The kinetics of acicular ferrite formation in reaustenitised weld metal of different chemical compositions. The effect of temperature was also considered.

(b) The morphology of acicular ferrite changes as a function of driving force and active nucleation site density. The aim was to rationalise of the microstructures observed in isothermally transformed specimens.

(c) Martensite and acicular ferrite have different properties. The strength and hardness of the mixed microstructures should therefore be dependent on the amount of acicular ferrite present. The fraction of each microstructural component was measured for isothermally transformed and quenched samples. Mean hardness values from each specimen were then correlated with the measured acicular ferrite content and the alloy chemistry. The yield strength of a mixed microstructure of acicular ferrite and martensite is expressed as

$$\sigma_y = V_{\alpha_a} \left(\sigma_{Fe} + \sum_i x_i \kappa_i + \Delta\sigma_{\text{mic}} \right) + (1 - V_{\alpha_a})\sigma_{\alpha'}$$

(where the notation is the same as in Chapter 6). The microstructural contribution of acicular ferrite to the overall hardness $\Delta\sigma_{\text{mic}}$ was determined, and the agreement between predicted and measured hardness was examined.

(d) The maximum amount of acicular ferrite that can form at any temperature increases with undercooling below the B_S temperature (Yang & Bhadeshia, 1987). The variation is expected to be consistent with the slope of the T_0' curve in the phase diagram. The measured volume fraction of acicular ferrite was compared with calculations for each alloy.

9.2 Experimental Method

Specimens of weld metal were cut from the undiluted heart of each weld and swaged down to 8 mm diameter rods. The rods were homogenised by sealing in quartz tubes under a partial pressure of pure argon and holding for 3 days at 1200°C before water quenching. The outer layers of the rods were then removed by turning down to a diameter of 6 mm. Dilatometry was carried out on a THERMECMASTOR thermo-mechanical simulator (TMS). A large austenite grain size was required in order to enhance the formation of acicular ferrite. An austenitisation treatment of 1 minute at 1350°C was found to be adequate in this respect, with little or no grain boundary nucleated bainite being observed in the transformed specimens. After austenitisation the specimens were cooled to the isothermal transformation temperature at $40°Cs^{-1}$ and held there for five minutes before quenching to room temperature with nitrogen gas. This was found to give the optimum compromise cooling rate that minimised the undershooting of the isothermal hold temperature whilst at the same time ensured the absence of transformation during the quench. As will be explained later, the undershooting of the test temperature on cooling *did* prove to be a major obstacle in producing accurate quantitative data for the early stages of transformation. For scanning electron microscopy, specimens were cut, mounted and polished using standard metallographic techniques, then given a medium/deep etch in 2% nital. Hardness testing was performed using a Vickers pyramidal indenter (load 10 kg) on lightly etched samples. The mean of five measurements was taken for each sample.

9.3 Results

Figures 9.1-9.3 show the dilatometric results from isothermal transformation experiments at a variety of temperatures, for each alloy in the high strength weld metal series. The figures show plots of relative radius change, $\Delta r/r$ versus time. Examples of the acicular ferrite morphology in the transformed specimens are shown for alloys 118 and 115 in Figures 9.4-9.6 and Figures 9.7-9.9 respectively. Alloy 118 is the low nickel variant of the alloy series, with alloy 115 being the high manganese variant. These alloys were selected for display since they most clearly illustrate the trends in microstructure shown by the welding alloys as the transformation temperature was varied. In Figures 9.10, 9.11 and 9.12, the experimentally measured volume fractions of acicular ferrite observed in the transformed specimens are compared with theory, assuming transformation stops when the austenite carbon content reaches $x_{T_0'}$. The $x_{T_0'}$ composition was determined using theory outlined in Chapter 2. A comparison of the predicted and experimentally measured hardness values (after optimising the microstructural strength contribution of acicular ferrite) is shown in Figure 9.13. The optimum value of the microstructural contribution of acicular ferrite to the overall specimen hardness was found to be

$$\Delta\sigma_{\mathrm{mic}} = 352 \pm 20 \text{ MPa} \tag{9.1}$$

9.4 Discussion

9.4.1 Transformation Kinetics

It must be noted that after quenching, the duration of the undershoot below the desired isothermal transformation temperature was around 4 seconds on average, meaning that the results shown in Figures 9.1-9.3 are not truly representative of the *early* stages of the transformation since ferrite formation and thermal expansion are occurring simultaneously. It proved impossible to fit the transformation data to the model presented in Chapter 3, the disagreement between prediction and experiment at the early stages of transformation dominating the error, resulting in poor overall agreement, and unsatisfactory determination of the empirical constants of the model. In all the isothermal runs the relative radius change reading decreased momentarily shortly after it reached its maximum value, as can be seen clearly in some of the experimental data. The magnitude of this effect was not identical in all specimens, nor did it always occur at the same time. Examination of the microstructures of the transformed specimens showed little change across the specimen diameter, suggesting that if this effect was due to thermal contraction of the specimen core, which was at a higher temperature than the exterior during transformation, the effect on the resultant microstructure was negligible. It is conceivable however, that the transformation rate of the core region might differ from that of the exterior if such temperature gradients did exist in the specimen.

It is noteworthy that the transformation rates of all alloys are similar, depending mainly on the undercooling of each alloy below its respective B_S temperature, despite the fact that the predicted B_S temperatures themselves vary by around 70°C (*c.f.* alloy 114 and alloy 116). If W_S represents the highest temperature at which nucleation of bainite is possible, and that at this temperature there is a minimum nucleation rate, the kinetics of transformation to bainite or acicular ferrite are determined primarily by the undercooling below W_S. (In most of the welding alloys considered here W_S and B_S are identical *i.e.* transformation is nucleation limited.) The observation that at similar undercooling below W_S the reaction kinetics are similar for all the welding alloys, despite differences in substitutional solute content, supports the assertion that all alloys have the same nucleation rate at W_S (Bhadeshia 1981a). It is therefore also consistent with the modified bainite kinetics model presented in Chapter 3. The small differences in the carbon contents of the alloys ensure that autocatalytic effects are similar despite their different substitutional solute content.

9.4.2 Morphology of Acicular Ferrite in Isothermal Transformed Specimens

The isothermal transformation temperatures used were chosen in order to investigate the nature of acicular ferrite formation at small driving forces and therefore low nucleation rates. It is interesting to note that at the smallest undercoolings (Figures 9.6 and 9.9) both alloy 118

and alloy 115 show a marked tendency for sheaf formation, which decreases somewhat as the driving force increases. Undoubtedly, at low driving forces, the significance of each nucleation event on an inclusion is increased, enabling subsequent auto-catalytic nucleation to dominate the eventual microstructure, since when nucleation rate is low there is less impingement between plates nucleated on neighbouring sites. Since the auto-catalytic nucleation occurs on previously formed plates, it is reasonable to assume that, given the opportunity, the plates will align in a manner similar to bainite sheaves. At higher driving forces (Figures 9.4, 9.5, 9.7 and 9.8) when the nucleation frequency is higher, the resulting hard impingement between plates stifles sheaf formation, though alloy 118 transformed at 500 °C continues to show some sheaves (Figure 9.4). Transformed at 450°C alloy 115 shows a conventional acicular ferrite microstructure.

The apparent variation of plate size in the microstructure of alloy 118 transformed at 500°C and 510°C (Fig. 9.4 and 9.5) is probably due to sectioning effects on plate arrays that show a high degree of alignment, suggesting that certain plate orientation variants are favoured.

The very clear contrast between the acicular ferrite and the inter-plate regions is probably due to the fact that during the isothermal transformation hold (5 minutes) there was ample time for complete carbon redistribution in the untransformed austenite, resulting in clear etching differences between the acicular ferrite and the subsequently formed martensite. It is possible that the inter-plate regions observed in the microstructure of alloy 118 transformed at 530 °C (Fig. 9.6) contain a fine dispersion of acicular ferrite plates, since carbon enrichment of the untransformed austenite would not have occurred to a great degree with such a small volume fraction of acicular ferrite being formed. The retardation of the acicular ferrite reaction by the partitioned carbon would therefore not be sufficient to prevent transformation during the post-isothermal hold quench. There is, however, no difficulty in distinguishing the acicular ferrite formed at the isothermal hold temperature from the inter-plate regions in the eventual microstructure.

Since it is believed that sheaves offer less resistance to crack propagation than dispersions of plates, as in acicular ferrite, the implications these results have for isothermally transformed inoculated steels are clear. If a fine, uniform acicular ferrite microstructure with a large fraction of martensite is desired this can best be achieved by partial transformation to acicular ferrite at a relatively low temperature *i.e.* interrupting the transformation before completion by quenching, rather than allowing complete transformation to the maximum allowable extent at a higher temperature at which sheaf formation tendency will increase.

9.4.3 Properties of Isothermally Formed Acicular Ferrite/Martensite Structures

The degree of agreement between the predicted and measured hardness of the isothermally transformed specimens supports the applicability of the model described in Chapter 6 for

predicting the hardness of mixed microstructures of acicular ferrite and martensite. Since the plate size of acicular ferrite and the sheaf morphology is slightly different in continuously cooled and isothermally transformed specimens it is unlikely that the microstructural strengthening component of acicular ferrite is the same in both cases. It must be noted however that there is also likely to be a variation in this term for specimens of each alloy transformed at different temperatures, since it is driving force differences that give rise to variations in plate size and sheaf forming tendency.

The best fit value for the microstructure strengthening term was however very close to the value determined in Chapter 5 for the as-deposited weld metals. When this optimised term is included in the model for overall hardness of the microstructure there is fair agreement between predicted and experimental results (Figure 9.13). The large amount of scatter in the results is perhaps a consequence of certain microstructures where, due to the low fraction of acicular ferrite formed during the isothermal hold, the formation of further small amounts of ferrite during the quench to martensite was unavoidable. In the point counting procedure, the areas obviously formed during isothermal treatment were counted as acicular ferrite and other regions classed as martensite, though in fact the martensite may be interspersed with fine acicular ferrite plates formed during the post isothermal-hold quench *e.g.* Figure 9.6. The small fractions of fine acicular ferrite formed during quenching could conceivably affect the overall hardness of the microstructure.

9.4.4 The Incomplete Reaction Phenomenon in Acicular Ferrite

As can be seen from Figures 9.10, 9.11 and 9.12 the measured volume fraction of acicular ferrite decreases dramatically as the B_S temperature is approached. This is despite the fact the transformation temperature is well inside the $\alpha + \gamma$ phase field. It is clear that the transformation mechanism is far from equilibrium. The acicular ferrite fractions formed by isothermal transformation are significantly lower than that predicted by assuming that reaction stops when the carbon content of the untransformed austenite reaches $x_{T_0'}$ or x_{N_0}. This discrepancy lies outside the statistical error limit of the volume fraction measurements ($\approx 10\%$) and even if it is assumed that acicular ferrite contains no carbon, the measured ferrite volume fraction of acicular ferrite still falls below the predicted value. Note that this is despite the fact that, as shown in Chapter 8, the steels are observed to transform to acicular ferrite and bainite above the predicted B_S temperatures, as is confirmed by certain isothermal transformation results presented here. In such cases the measured volume fraction is obviously greater than the predicted value.

Undershooting the isothermal transformation temperature might also be expected to increase the amount of acicular ferrite by boosting nucleation at the earlier stages of transformation. The measured acicular ferrite fractions of acicular ferrite are lower than theory predicts

despite this effect as well.

A possible reason for the phenomenon is that the build up of stresses in the austenite around plates of acicular ferrite hinders the late stages of transformation. This is despite the fact that indications are that it is easier to nucleate acicular ferrite and bainite in these welding alloys than in conventional wrought steels, as discussed in Chapter 8.

9.5 Conclusions

The kinetic data from isothermal transformation of the high strength welding alloys supports the theoretical prediction that the rate of reaction is determined mainly by the undercooling below the B_S temperature. Quantitative optimisation of a model for acicular ferrite kinetics was not possible since the undershooting of the isothermal transformation temperature interfered with the dilatometric data at early stages of transformation.

The microstructure of the isothermally transformed specimens illustrates the importance of driving force on the development of sheaves from the initial nucleation events on inclusions. At higher driving forces the tendency to form sheaves decreases. The extent of transformation measured in the the experimental specimens indicates that the prediction of the limiting acicular ferrite volume fraction using the $x_{T_0'}$ curve is a consistent overestimate.

Prediction of the hardness of microstructures consisting of a mixture of acicular ferrite and martensite by estimating the contributions of the microstructural constituents to the overall hardness is found to be in broad agreement with the measured values.
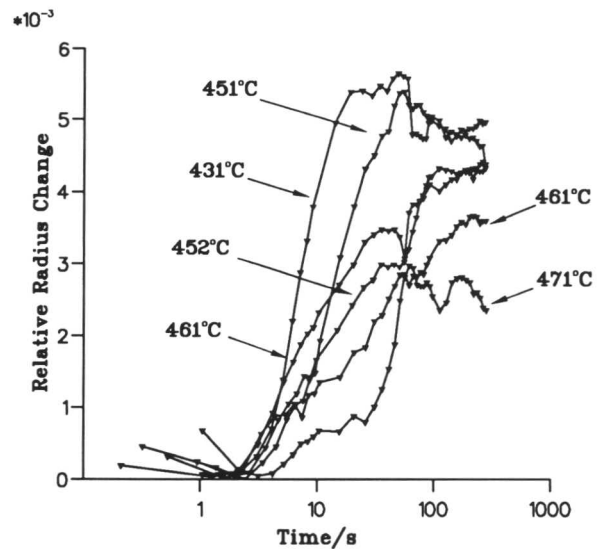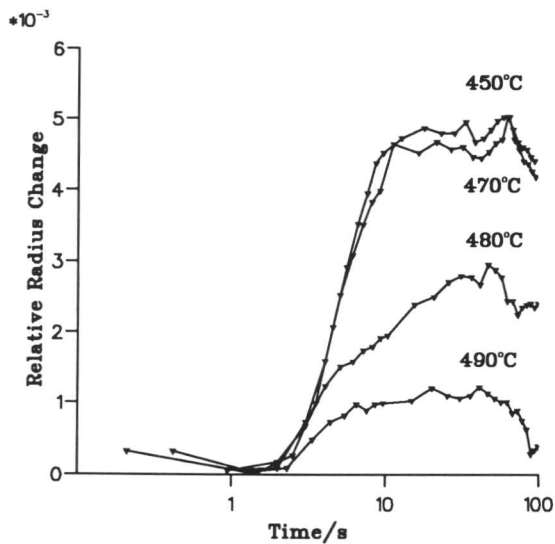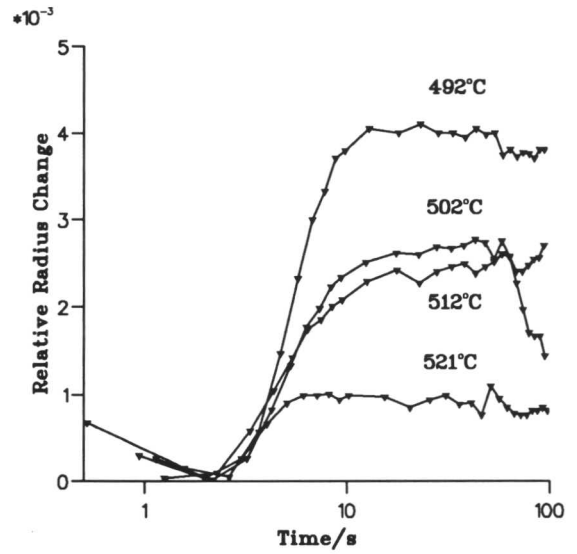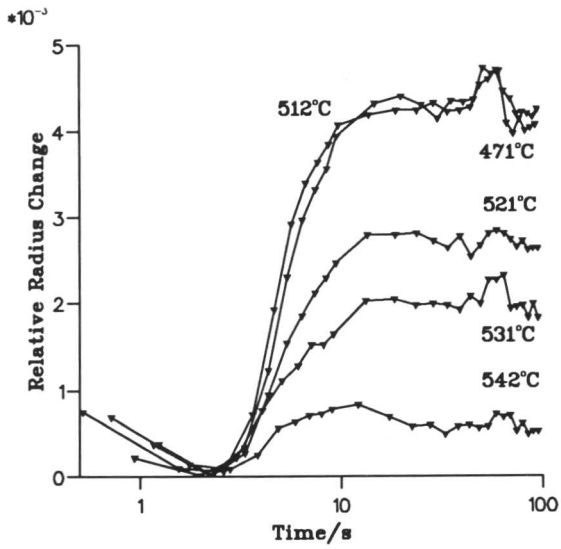
Figure 9.1 Isothermal transformation kinetics data for (a) alloy 112 (b) alloy 113 (c) alloy 114 (d) alloy 115. The transformation temperatures of each run are indicated on the plots.
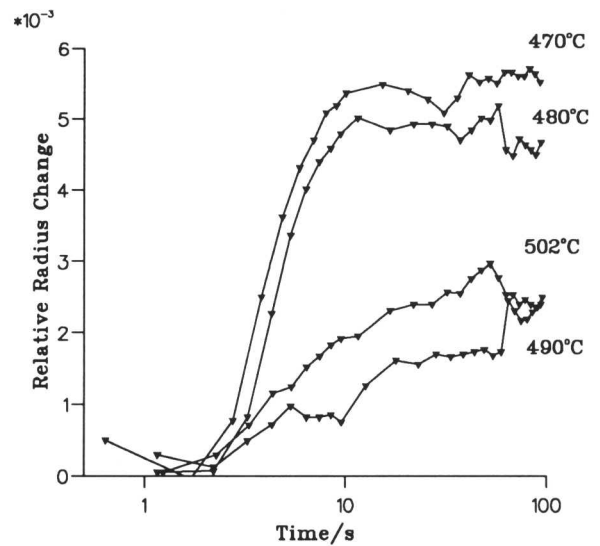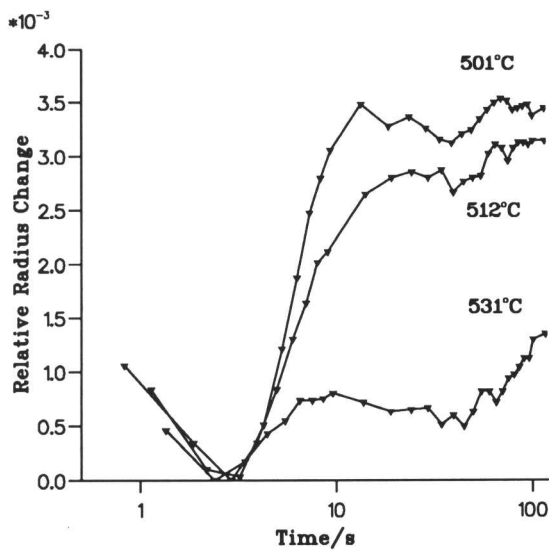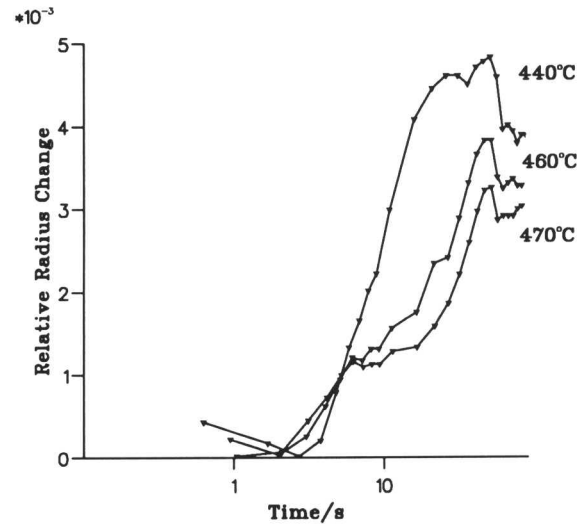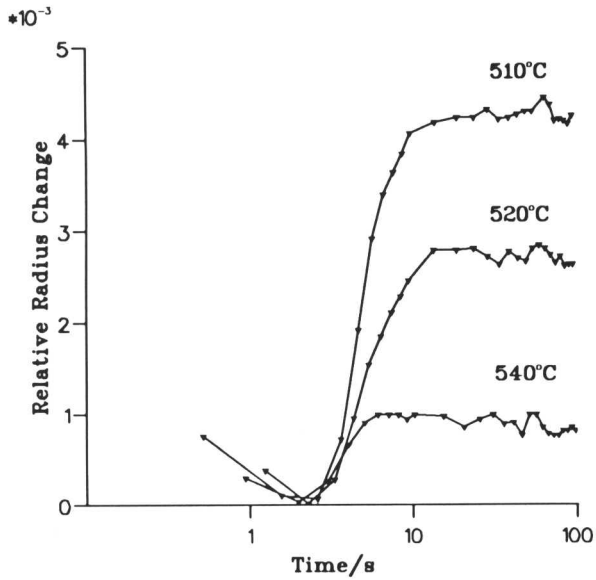
Figure 9.2 Isothermal transformation kinetics data for (a) alloy 116 (b) alloy 117 (c) alloy 118 (d) alloy 119. The transformation temperatures of each run are indicated on the plots.
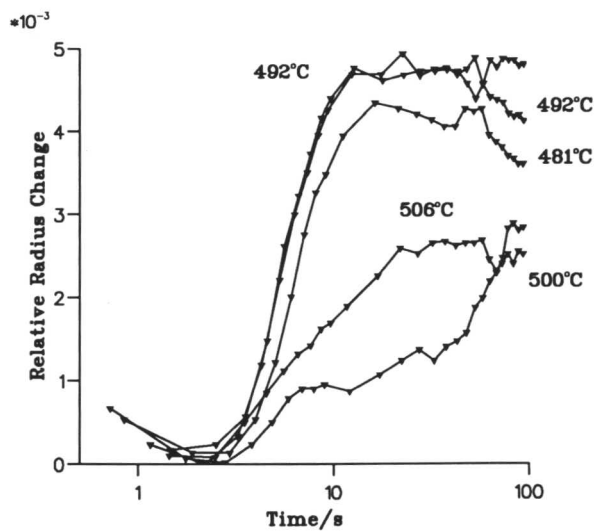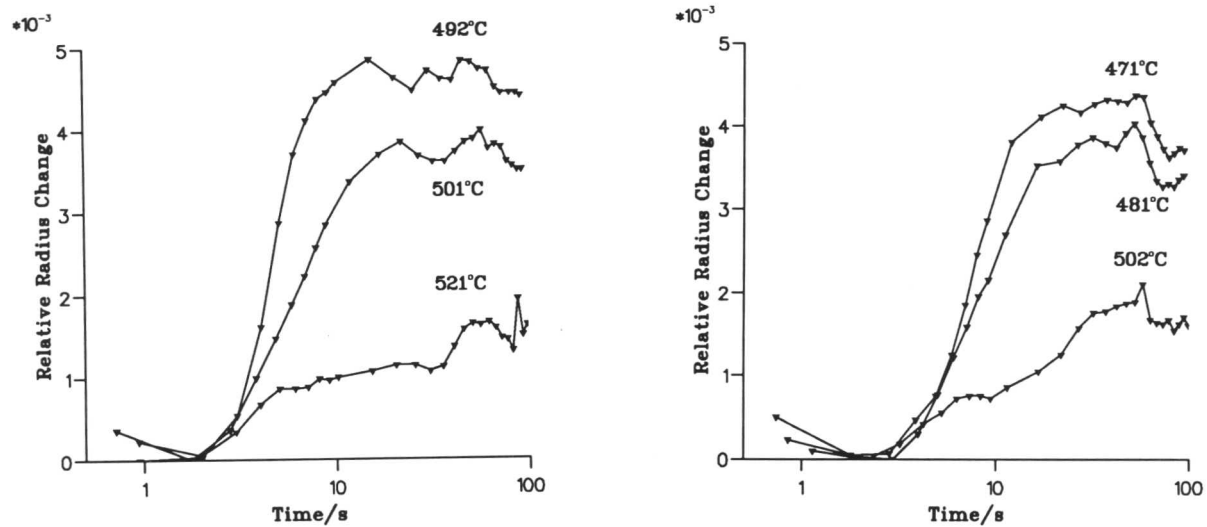
Figure 9.3 Isothermal transformation kinetics data for (a) alloy 120 (b) alloy 121 (c) alloy 122. The transformation temperatures of each run are indicated on the plots.
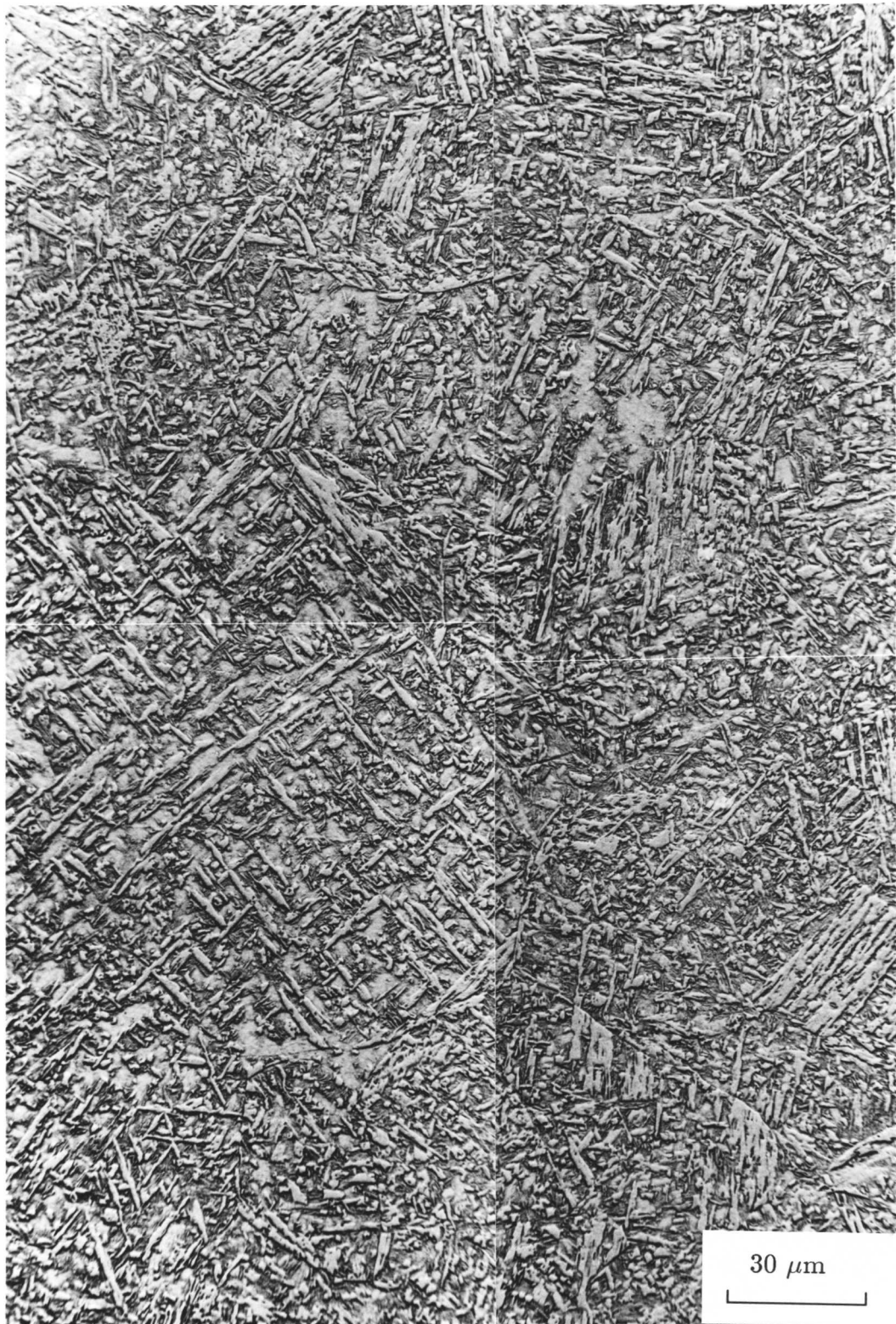
Figure 9.4 The microstructure of alloy 118 isothermally transformed for five minutes at 500°C after austenitisation for 1 minute at 1350°C. Acicular ferrite plates appear raised, and are clearly distinguishable from surrounding martensite.
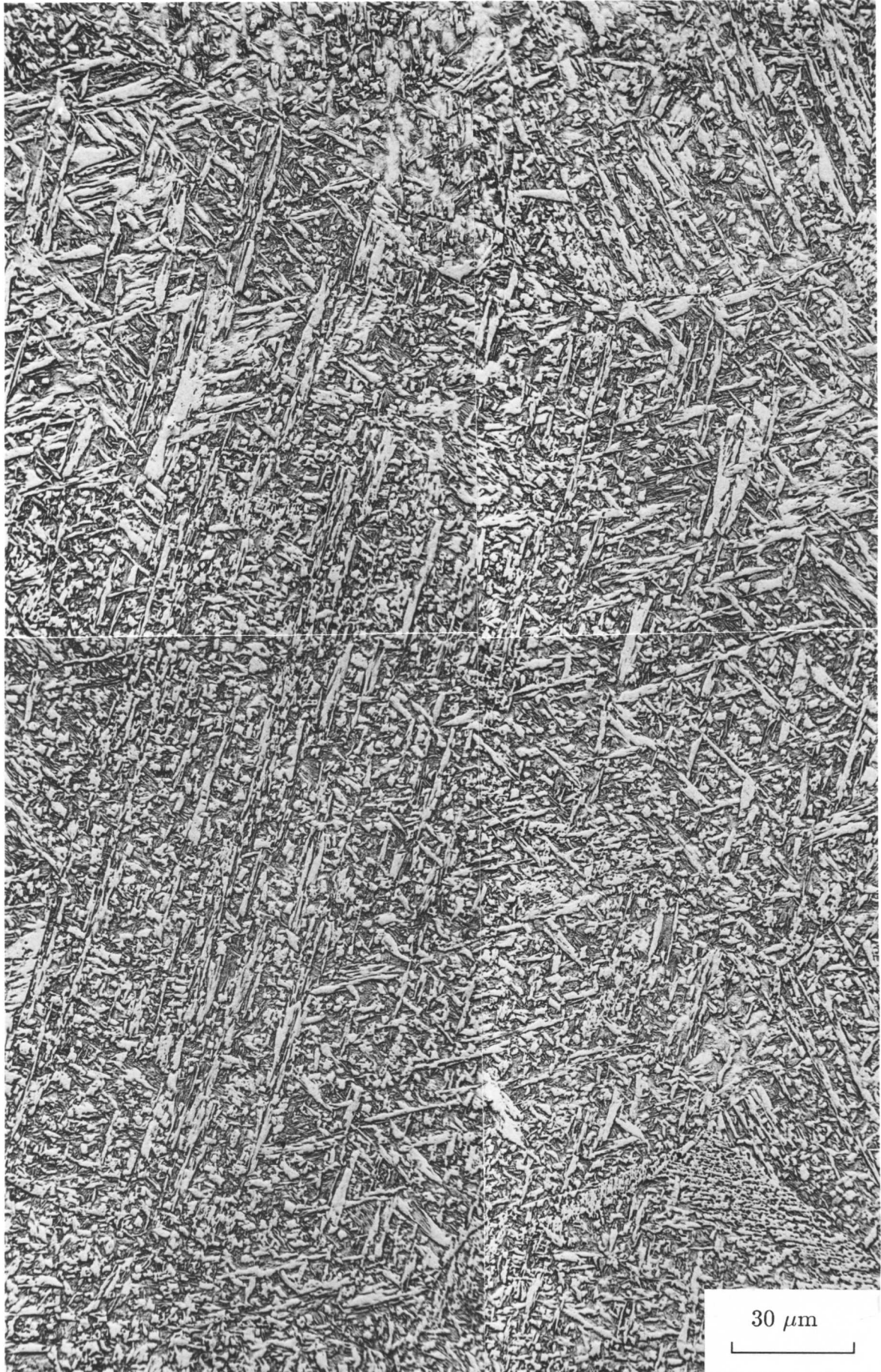
Figure 9.5 The microstructure of alloy 118 isothermally transformed for five minutes at 510°C after austenitisation for 1 minute at 1350°C. The acicular ferrite shows an increased tendency to form sheaves (arrowed).
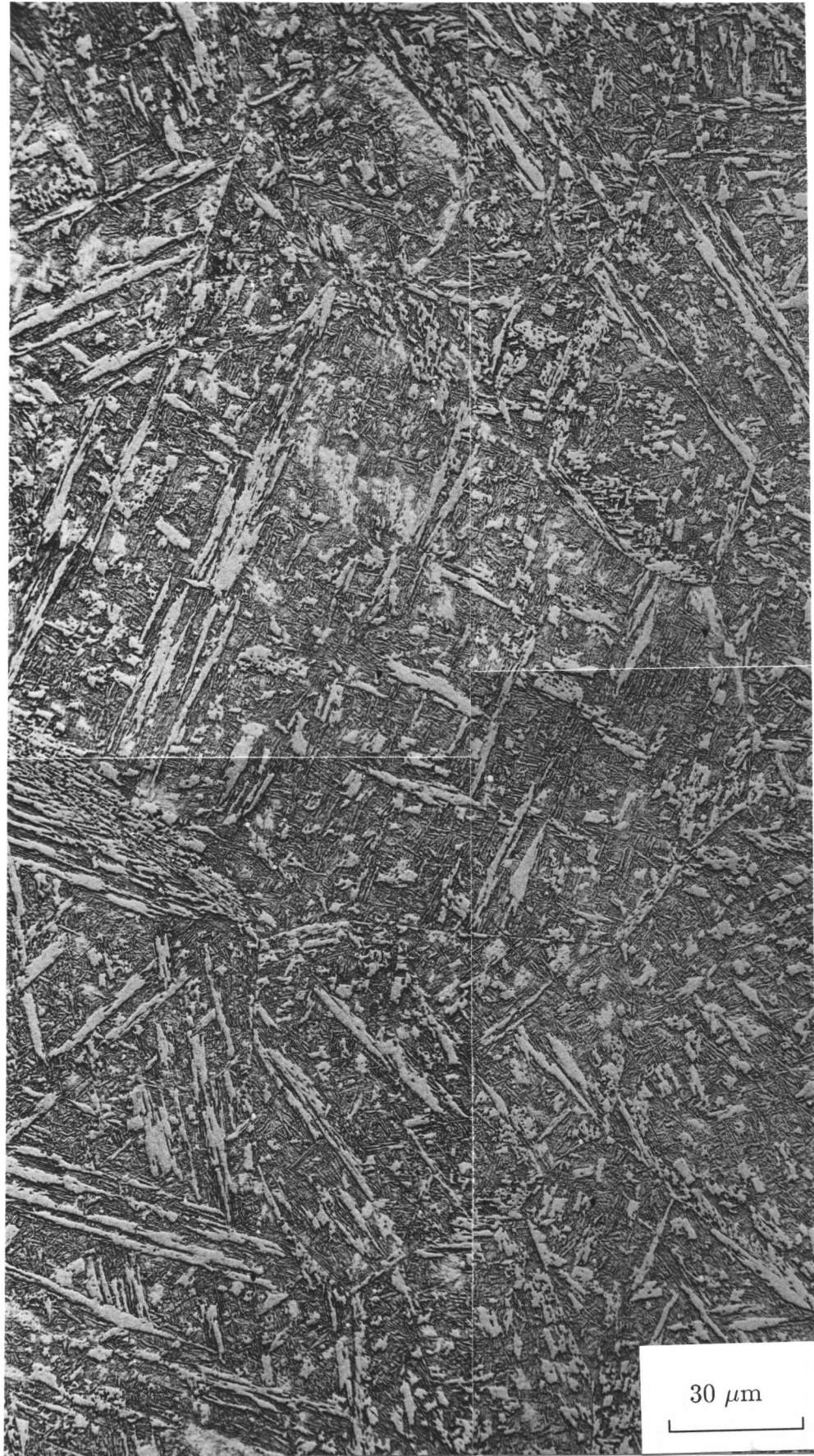
Figure 9.6 The microstructure of alloy 118 isothermally transformed for five minutes at 530°C after austenitisation for 1 minute at 1350°C. Sheaf formation is very pronounced.

30 μm
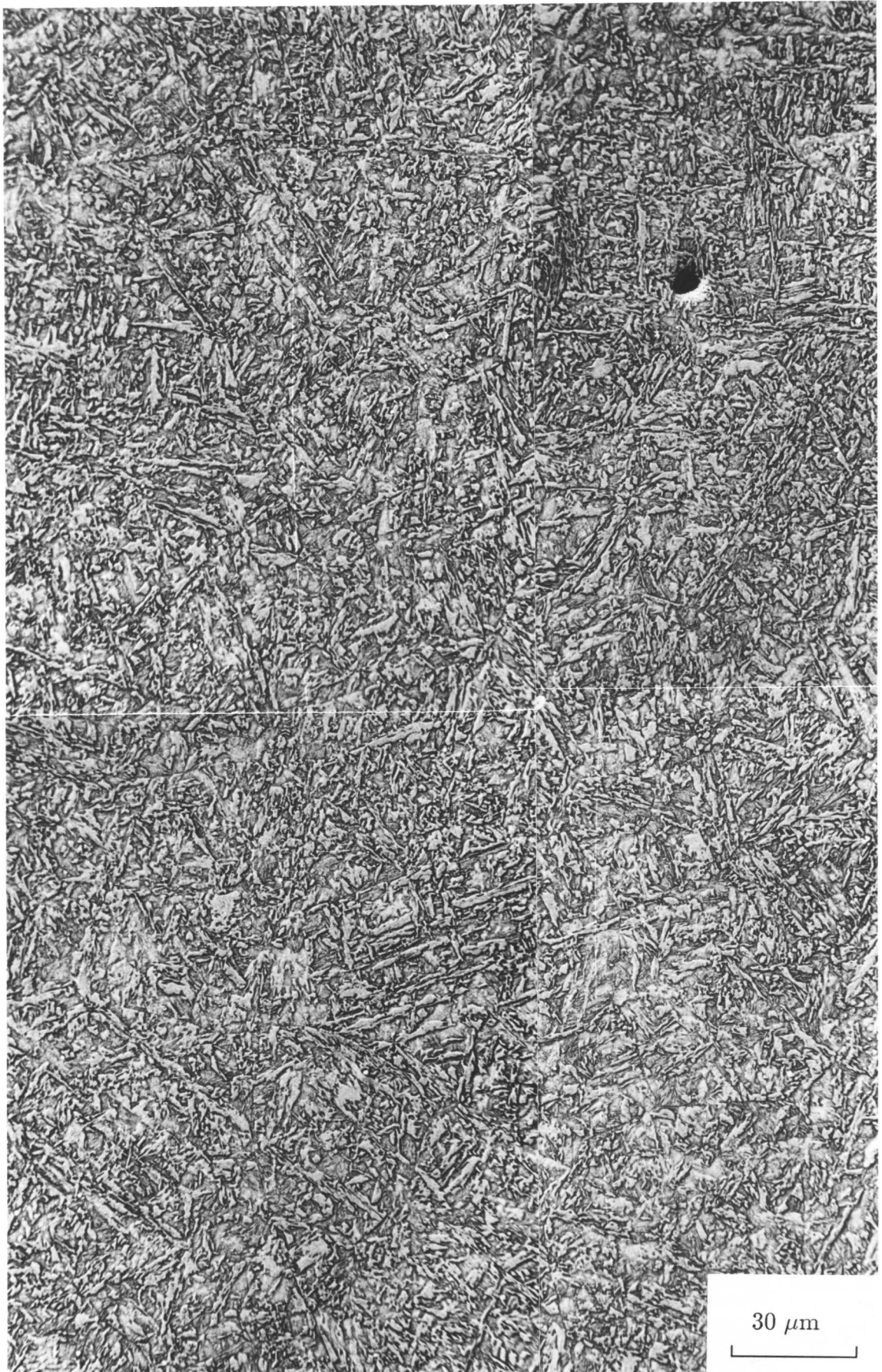
Figure 9.7 The microstructure of alloy 115 isothermally transformed for five minutes at 450°C after austenitisation for 1 minute at 1350°C. The tendency to form sheaves is slight.
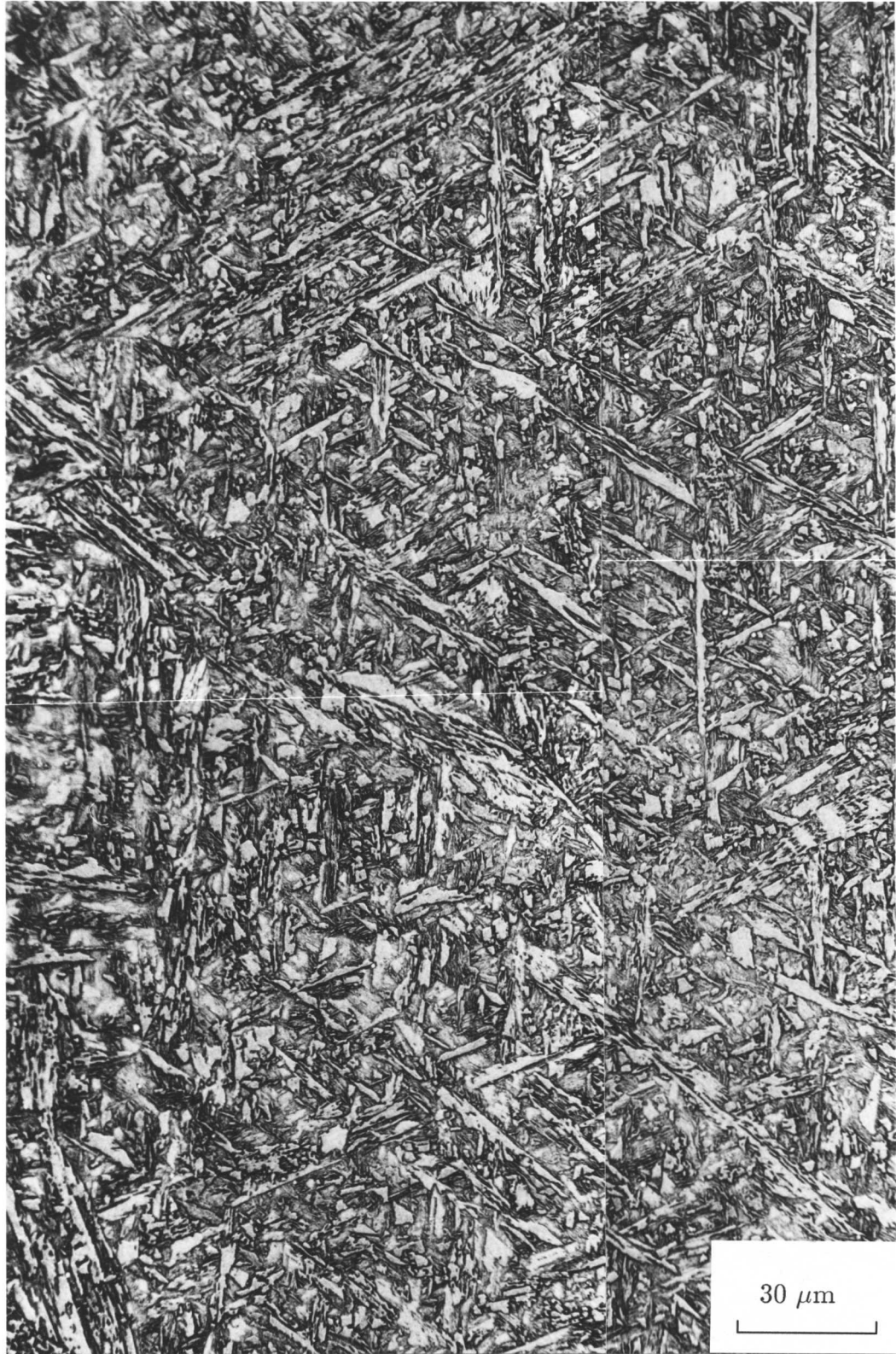
Figure 9.8 The microstructure of alloy 115 isothermally transformed for five minutes at 460°C after austenitisation for 1 minute at 1350°C. There is a profound increase in sheaf forming tendency (arrowed), and some plate orientations appear favoured.

162

30 μm

Figure 9.9 The microstructure of alloy 115 isothermally transformed for five minutes at 470°C after austenitisation for 1 minute at 1350°C. The acicular ferrite fraction is very low, therefore sheaf formation is pronounced (arrowed).

163
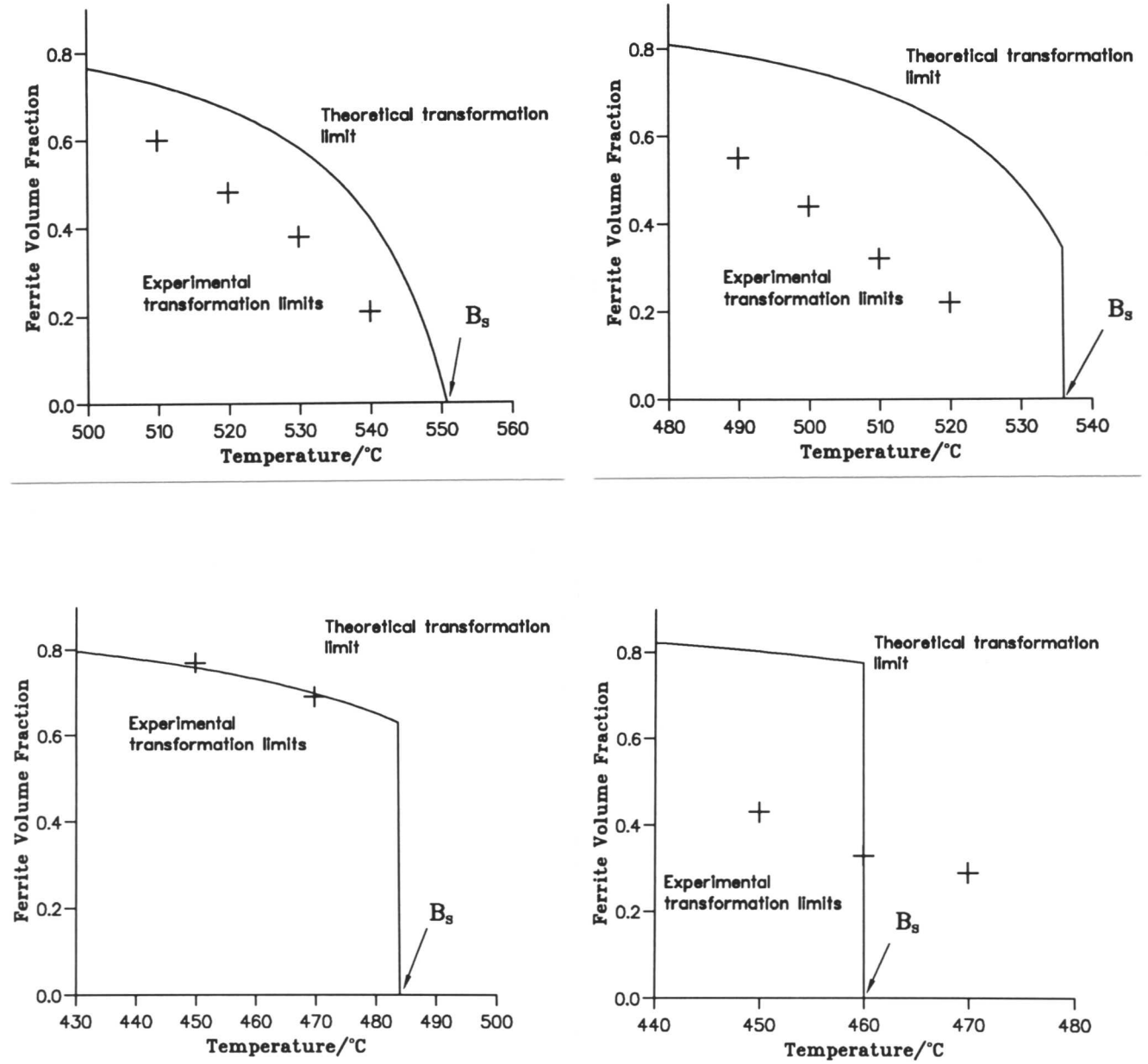
Figure 9.10 Comparison of predicted and measured volume fractions of acicular ferrite for different isothermal transformation temperatures: (a) alloy 112 (b) alloy 113 (c) alloy 114 (d) alloy 115.

164
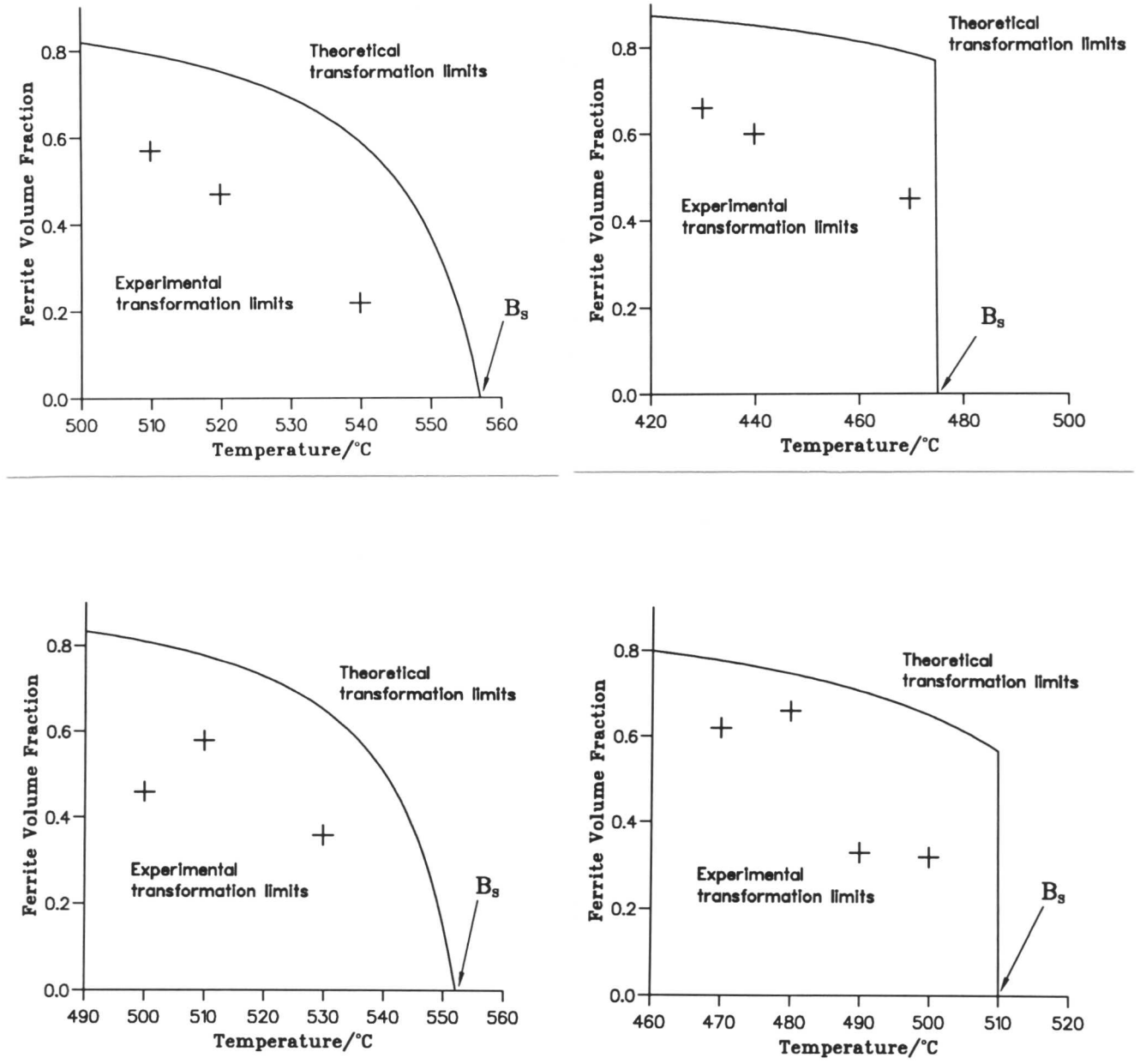
Figure 9.11 Comparison of predicted and measured volume fractions of acicular ferrite for different isothermal transformation temperatures: (a) alloy 116 (b) alloy 117 (c) alloy 118 (d) alloy 119.
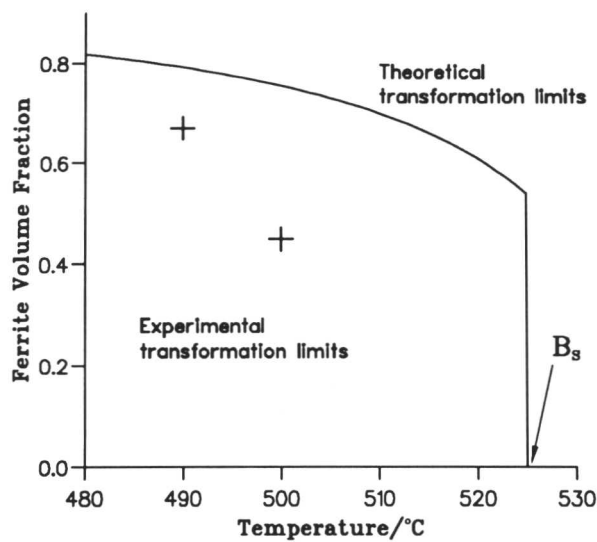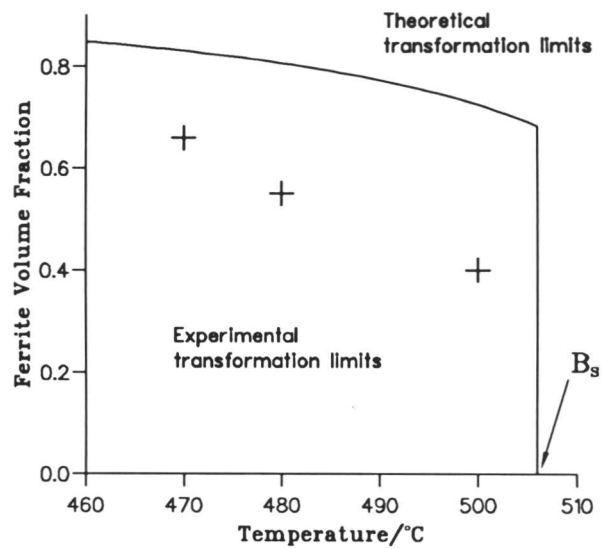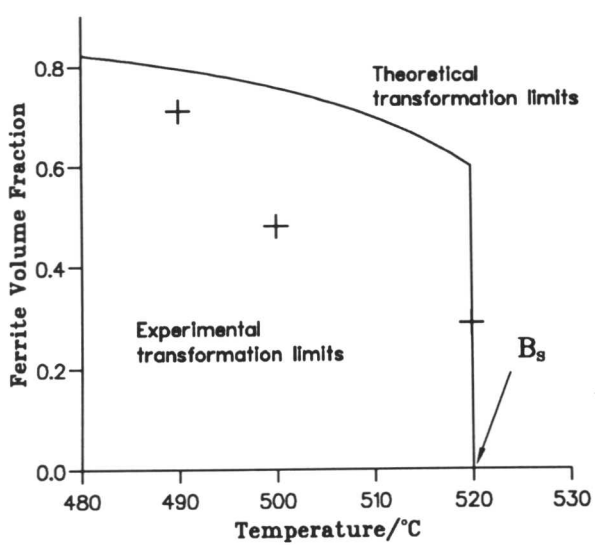
Figure 9.12 Comparison of predicted and measured volume fractions of acicular ferrite for different isothermal transformation temperatures: (a) alloy 120 (b) alloy 121 (c) alloy 122

166
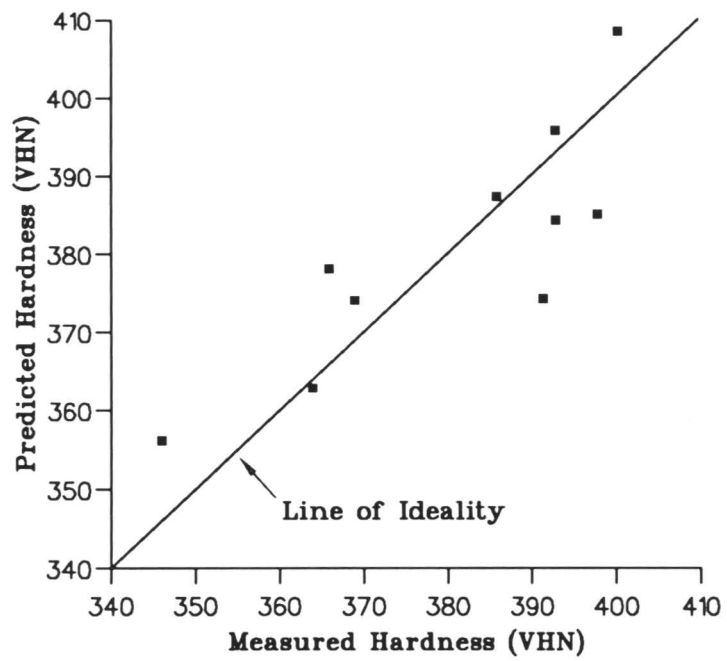
Figure 9.13 Comparison of predicted and experimentally measured hardness values of the isothermally transformed specimens from the welding alloy series.

CHAPTER 10

Future Work

10.1 Further Application of Present Work

Many of the experimental and theoretical tools developed during this work can be applied in a general way to other materials and under different conditions. Computer algorithms have been developed that will enable the analysis of new data on bainite kinetics and optimisation of the model refined during the course of this study. In this way it will be possible to identify trends previously unaccounted for, which will stimulate further research in the field. It has also been demonstrated that use of SEM enables more meaningful quantification of high strength microstructures, which will aid the improvement of quantitative models of microstructure development and mechanical properties.

10.2 New Work

Many topics which would be essential to and eventual comprehensive model of weld microstructure development have not been considered. The quantitative analysis of the continuous cooling transformation to acicular ferrite is an example. In principle it is possible to analyse the dilatometric data obtained during continuous cooling to give volume fraction data versus time and temperature. Computer programs have been developed to analyse the data and determine best fit constants for the bainite model under these conditions. Difficulties arise however in accounting for the variation in the expansion coefficient of austenite with cooling rate. It would certainly be of interest however to identify trends in the microstructures produced in the alloys considered in this work under fast cooling conditions.

Extraction replica TEM work would enable the analysis and quantification of the inclusion content and size distribution in the weld metal. In the absence of other contributory factors this inclusion distribution will have and important effect on the nucleation rate of acicular ferrite. It will be of great interest to investigate whether the measured compositions of the active inclusions support the conclusions of recent work at Cambridge on the mechanism of nucleation on inclusions (Gregg, 1992).

APPENDIX 1

Analysis of Dilatometric Data

Data from the dilatometer and thermo-mechanical simulator is output as relative length change $\Delta l/l$ (or relative readius change $\Delta r/r$), temperature and time. In order to monitor the development of the ferrite volume fraction during isothermal transformation it is necessary to analyse the length change data.

Let a_α, a_γ and $a_{\overline{\gamma}}$ represent the lattice parameter of carbon-free ferrite, austenite of a carbon mole fraction x_γ and austenite of bulk alloy carbon mole fraction $\overline{x}$. Assuming isotropic dilatation in a polycrystalline test specimen, the relative length change (or relative radius change) can be related to the relative volume change $\Delta V/V$

$$\frac{\Delta V}{V} = \frac{\Delta l}{l} + 2\frac{\Delta r}{r} = 3\frac{\Delta l}{l}$$

After a volume fraction V_α of ferrite has formed

$$\frac{\Delta l}{l} = \frac{2V_\alpha a_\alpha^3 - (1 - V_\alpha) a_\gamma^3 - a_{\overline{\gamma}}^3}{3a_{\overline{\gamma}}^3}$$

The lattice parameter of austenite is calculated in the following way

$$a_\gamma = \left(a_0 + c_c x_\gamma + \sum_j c_j x_j\right) \left(1 + e_\gamma (T - 298)\right)$$

where

$$x_\gamma = \frac{\overline{x} - V_\alpha x_\alpha}{1 - V_\alpha}$$

and

$$a_\gamma = \left(a_0 + c_c \overline{x} + \sum_j c_j x_j\right) \left(1 + e_\gamma (T - 298)\right)$$

where a_0 is the lattice parameter of unalloyed austenite at room temperature, and c_c and c_j are the coefficients of contributions to lattice parameter of carbon and the ith substitutional alloying element.

The lattice parameter of ferrite at the reaction temperature is

$$a_\alpha = a_{\alpha 0} \left(1 + e_\alpha (T - 298)\right)$$

where $a_{\alpha 0}$ is the experimentally measured lattice parameter of carbon-free ferrite. e_γ and e_α are the experimentally determined linear thermal expansion coefficients of austenite and ferrite respectively. The equation relating $\Delta l/l$ with V_α can then be solved iteratively for each value of $\Delta l/l$, thereby describing the development of ferrite during the isothermal hold.

169

Bhadeshia (1982b) obtained the following values for e_α, e_γ and $a_{\alpha 0}$ for the three high-silicon steels used in his analysis of the isothermal transformation kinetics of bainite.

	Fe–Mn–Si–C	Fe–Ni–Si–C	300 M
e_α	0.13049×10^{-4} K^{-1}	0.11826×10^{-4} K^{-1}	0.11103×10^{-4} K^{-1}
e_γ	0.21151×10^{-4} K^{-1}	0.18431×10^{-4} K^{-1}	0.17591×10^{-4} K^{-1}
$a_{\alpha 0}$	2.8869 ± 0.002 Å	2.8650 ± 0.0016 Å	2.8661 ± 0.001 Å

APPENDIX 2

Program for Optimisation of Bainite Kinetics Constants

```
        PROGRAM MAIN
        IMPLICIT DOUBLE PRECISION (A-H,L-Z),INTEGER (I-K)
        DIMENSION CNT(4),IND(50)
```

. . . .

```
* junk is a disposable output file, wa contains the initial guess values
* for the constants. RTOT is the current best sum of squares error.
```

. . . .

```
        OPEN (UNIT=1,FILE='wa')
        open (unit=3,file='theory/geff6/junk')
        ILIM=1
        CALL IDENTIFY(IND,ID)
        READ (1,*) (CNT(J1),J1=1,4),RTOT
        WRITE (3,*) CNT(4)
        CALL MINIMISE(CNT,RTOT,IND,ID,ILIM)
        END
```

. . . .

```
* This subroutine identifies the individual dataruns in the
* set and arranges them in a two dimensional array
```

. . . .

```
        IDENTIFY (INDR,IDR)
        IMPLICIT DOUBLE PRECISION (A-H,L-Z),INTEGER (I-K)
        COMMON /ONE/ TKI(75,50),VNI(75,50),TIMI(75,50),THI(75,50)
        COMMON /TWO/ FMI(75,50),NDI(75,50),WSI(75,50),XBI(75,50)
        DIMENSION INDR(50)
        IDR=1
        IVDR=0
        PRE=0.0d0
        DO  10 I1=1,5000
           J2=0
           READ (5,*,END=11) AA,BB,CC,DD,EE,FF,GG,HH
           IF (BB .GT. PRE) THEN
              IF (I1 .EQ. 1) IVDR=0
              IVDR=IVDR+1
              PRE=BB
           ELSE
              PRE=0.0
              IDR=IDR+1
              IVDR=1
           ENDIF
           VNI(IDR,IVDR)=AA
           TIMI(IDR,IVDR)=BB
           THI(IDR,IVDR)=CC
           FMI(IDR,IVDR)=DD
           TKI(IDR,IVDR)=EE
           NDI(IDR,IVDR)=FF
```

```
                WSI(IDR,IVDR)=GG+273.15
                XBI(IDR,IVDR)=HH
                INDR(IDR)=IVDR
10          CONTINUE
11          INDR(IDR)=IVDR
            END
```

. . . .

* This subroutine adjusts the constants in turn and adopts any
* favourable changes

. . . .

```
            MINIMISE(CNT,TOT,IMND,IMD,ILIM)
            IMPLICIT DOUBLE PRECISION (A-H,L-Z),INTEGER (I-K)
            COMMON /ONE/ TKM(75,50),VNM(75,50),TIMM(75,50),THM(75,50)
            COMMON /TWO/ FMM(75,50),NDM(75,50),WSM(75,50),XBM(75,50)
            DIMENSION CNT(4),CDUM1(4),CDUM2(4),IMND(50)
            IIT=0
            IGO=0
            DO  10 IDUM=1,4
                CDUM1(IDUM)=CNT(IDUM)
                CDUM2(IDUM)=CNT(IDUM)
10          CONTINUE
1           DO 30 I1=1,4
                PARA=0.3D0
2               CDUM1(I1)=(1.0D0+PARA)*CNT(I1)
                CDUM2(I1)=(1.0D0-PARA)*CNT(I1)
                CALL SUMSQ(CDUM1,SUM1,IMND,IMD,IGO)
                CALL SUMSQ(CDUM2,SUM2,IMND,IMD,IGO)
                IF (SUM1 .LT. TOT) THEN
                    TOT=SUM1
                    CNT(I1)=CDUM1(I1)
                    WRITE (3,999) (CNT(J1),J1=1,4),TOT
                    IIT=IIT+1
                    IF (IIT .GE. ILIM) GOTO 31
                ENDIF
                IF (SUM2 .LT. TOT) THEN
                    TOT=SUM2
                    CNT(I1)=CDUM2(I1)
                    WRITE (3,999) (CNT(J1),J1=1,4),TOT
                    IIT=IIT+1
                    IF (IIT .GE. ILIM) GOTO 31
                ENDIF
                IF (PARA .GT. 1.0D-07) THEN
                    PARA=0.3D0*PARA
                    GOTO 2
                ENDIF
30          CONTINUE
31          IF (IIT .LE. ILIM) THEN
                GOTO 1
            ELSE
```

```
                 IGO=1
                 CALL SUMSQ(CNT,SUM1,IMND,IMD,IGO)
           ENDIF
999          FORMAT (' ',5D15.5)
           END

. . . . . . . . . . . . . . . . . . . . . . . . . . . . . . . . . . . . .
* This soubroutine calculates the sum of squares error between the
* predicted and measured reaction times
. . . . . . . . . . . . . . . . . . . . . . . . . . . . . . . . . . . . .
           SUMSQ(CD,SUMM,ISND,ISD,IGO)
           IMPLICIT DOUBLE PRECISION (A-H,L-Z),INTEGER (I-K)
           COMMON /ONE/ TKS(75,50),VNS(75,50),TIMS(75,50),THS(75,50)
           COMMON /TWO/ FMS(75,50),NDS(75,50),WSS(75,50),XBS(75,50)
           DIMENSION CD(4),ISND(50)
           SUMM=0.0D0
. . . . . . . . . . . . . . . . . . . . . . . . . . . . . . . . . . . . .
* This subroutine will calculate the sum total error for
* each datarun DSUM. The overall total is then returned as SUMM
. . . . . . . . . . . . . . . . . . . . . . . . . . . . . . . . . . . . .
           DO  10 I1=1,ISD
               DSUM=0.0D0
               DELT=0.0D0
               DO  20 I2=1,ISND(I1)
                   T=TKS(I1,I2)
                   GM0=FMS(I1,I2)
                   VNM=VNS(I1,I2)
                   TH=THS(I1,I2)
                   ND=NDS(I1,I2)
                   WSK=WSS(I1,I2)
                   XB=XBS(I1,I2)
                   VN2=VNS(I1,I2)
. . . . . . . . . . . . . . . . . . . . . . . . . . . . . . . . . . . . .
* TEFF1 time to form the previous measured fraction at this temp
* TEFF2 time to form thepresent fraction at this temp
* DELT is the effective time increment
* DELT is the predicted reaction time for the present fration
. . . . . . . . . . . . . . . . . . . . . . . . . . . . . . . . . . . . .
                   TEFF2=NEWF(T,GM0,VN2,TH,ND,CD,WSK,XB)
                   L1=DLOG(TEFF2)
                   L2=DLOG(TIMS(I1,I2))
                   DSUM=DSUM+(L1-L2)**2
                   IF (IGO .EQ. 1) THEN
                       OPEN (UNIT=7,FILE='junk1.dat')
                       OPEN (UNIT=8,FILE='junk2.dat')
                       OPEN (UNIT=9,FILE='junk3.dat')
                       IF (ND .EQ. 46.7D0) IOUT=7
                       IF (ND .EQ. 51.975D0) IOUT=8
                       IF (ND .EQ. 86.00D0) IOUT=9
                       WRITE (IOUT,999) TIMS(I1,I2),TEFF2
```

173

```
              ENDIF
20            CONTINUE
              SUMM=SUMM+DSUM
10            CONTINUE
999           FORMAT (' ',2F15.6)
              END
```

. . . .
* This function is the corrected theory presented in Chapter 3
. . . .

```
              DOUBLE PRECISION FUNCTION
      &    NEWF (TK,GM0,PSI,THETA,ND,CD,WSS,XB)
              IMPLICIT DOUBLE PRECISION (A-H,L-Z),INTEGER (I-K)
              PARAMETER (R=8.314D0,RR=2540D0)
              DIMENSION CD(4)
              C1=CD(1)
              BETA=CD(2)*(1.0D0- CD(4)*XB)
              C2=CD(3)
              GSM=ND
              GNT= 3.636*(TK-273.15) -2540D0
              GNW= 3.636*(WSS-273.15) -2540D0
              GAMMA= C2*(GM0-GNT)/(RR*R*TK)
              LL =LOGS(PSI,GAMMA,BETA,THETA)
              E = DEXP(-C2/(R*TK) -C2*GM0/(RR*R*TK))
              NEWF = C1*GSM*THETA*LL/E
              END

              DOUBLE PRECISION FUNCTION LOGS(PSI,GAMMA,BETA,THETA)
              IMPLICIT DOUBLE PRECISION (A-H,L-Z)
              IMPLICIT INTEGER (I-K)
              A=DEXP(-GAMMA)/(1D0+BETA*THETA)
              C=CT(GAMMA,BETA,THETA)/CB(GAMMA,BETA,THETA)
              B= 1D0-A-C
              LOGS=(B/(BETA*THETA))*DLOG(1D0+BETA*THETA*PSI)
      &    (-A*DLOG(1D0-PSI) -(C/GAMMA)*(DEXP(-PSI*GAMMA)-1D0))
              END

              DOUBLE PRECISION FUNCTION CT(GAMMA,BETA,THETA)
              IMPLICIT DOUBLE PRECISION (A-H,L-Z)
              IMPLICIT INTEGER (I-K)
              CT=1D0-DEXP(GAMMA/BETA)*(1D0-(1D0/BETA))
      &    -DEXP((GAMMA/BETA) -GAMMA)*((1D0/(BETA*(1D0+BETA*THETA)))
      &    + (THETA/(1D0+BETA*THETA)))
              END

              DOUBLE PRECISION FUNCTION CB(GAMMA,BETA,THETA)
              IMPLICIT DOUBLE PRECISION (A-H,L-Z)
              IMPLICIT INTEGER (I-K)
              CB=(1D0-1D0/BETA)*(1D0+THETA-DEXP(GAMMA/BETA))
              END
```

APPENDIX 3

Program for Predicting Bainite Transformation Kinetics

```
* At present the program is set to give isothermal kinetics for
* temperature in increments of 25 K above MS

        IMPLICIT DOUBLE PRECISION(A-H,L-Z),INTEGER(I-K)
        DIMENSION TC(1000),XT0(1000),GM0(1000),AE3(1000),X44(1000)
        DIMENSION CNS(4),THOLD(4)
        PARAMETER (S=0.69D-03)
        COMMON WS,GSM,CNS(4)

* Open the output files
        open (unit=1,file='wa1.dat')
        open (unit=2,file='wa2.dat')
        open (unit=3,file='wa3.dat')
        open (unit=4,file='wa4.dat')

        GSM=50.0

* Read the transformation start temperatures from the thermo file
        READ(5,*) IA
        READ (5,*)
        READ (5,*) WS,BS,MS,XB

* Open and read constants form the constants file
        OPEN (UNIT=7, file='theory/geff6/c')
        READ (7,*) (CNS(J1),J1=1,4)

* Establish the temperstures to be considered
        DO  5 IH=1,4
            THOLD(IH)=INT(MS)+25.0D0*IH
5           CONTINUE

* Read the thermodynamic data for 200 - 700 degC
        DO  10 I1=1,999
            READ (5,*,END=11) TC(I1),XT0(I1),GM0(I1),AE3(I1),X44(I1)
10          CONTINUE

11          INUM=I1-1
            IH=1
            DO  20 I2=1,INUM


            Search for the desired temperatures
            IF (TC(I2) .EQ. THOLD(IH))THEN
```

```
                    TCC=TC(I2)
                    XT=XT0(I2)
                    GM=GM0(I2)
                    X4=X44(I2)
                    X3=AE3(I2)
```

* Ensure that we are below the bs temperature
```
                    IF ((X4 .LT. XB) .OR. (XT .LT. XB)) GOTO 31
```

* If trapping is accounted for, the relative thickness of the
* ferrite plates and austenite films must be specified.
```
21                  F=0.0D0
```

```
                    IOUT=IOUT+1
                    IF (IOUT .EQ. 5) IOUT=7
```

* Loop for taking the extent of transformation from 0 to theta
```
                    DO  30 P=0.01D0,0.999D0,0.01D0
                        T=NEWF(P,TCC,TH,GM,XB,X3,XT,F)
```

* At present output is set to the new theory. The previous theory
* (Bhadeshia 1982) can be chosen if desired.
* T2=OLDF(P,TCC,TH,GM)

```
                    WRITE (IOUT,999) P*TH,T,TCC
30                  CONTINUE
```

```
31                  IH=IH+1
                ENDIF
20      CONTINUE
```

```
99      FORMAT(' ',2D15.5,F15.5)
        END
```

```
        DOUBLE PRECISION FUNCTION NEWF(P,TC,THETA,FM,XB,X3,XT,F)
        IMPLICIT DOUBLE PRECISION (A-H,L-Z)
        IMPLICIT INTEGER(I-K)
        DIMENSION CNT(4)
        COMMON WS,GSM,CNT(4)
        PARAMETER (R=8.314D0,S=0.69D-03,RR=2540D0)
```

* Establish the maximum extent of transformation allowable
* either with trapping or wihtout.

```fortran
. . . . . . . . . . . . . . . . . . . . . . . . . . . . . .
      THETA=(XB-XT)/((S+F*X3) - XT*(1.0D0-F))
      BETA=CNT(2)*(1.0D0-CNT(4)*XB)
      C2=CNT(3)
      TK=TC+273.15d0
      BT=1D0+BETA*THETA
      BTP=1D0+BETA*THETA*P
      B1B=1D0-1D0/BETA
      GNT=3.636D0*TC-2450.0D0
      GAMMA= CNT(3)*(FM-GNT)/(RR*R*TK)
      DD=DEXP(GAMMA/BETA)
      A=DEXP(-GAMMA)/(BT)
      CT=1D0 - DD*(B1B +A*(1D0/BETA+THETA))
      CB=B1B*(1D0+THETA -DD)
      C=CT/CB
      B=1-A-C
      IF (BTP .LT. 0.0) THEN
          WRITE (6,*) THETA
          PAUSE '1+BETA*THETA*PSI ¡ 1'
      ENDIF
      EE=DEXP(-C2/(R*TK) -C2*FM/(RR*R*TK))
      LOGS=-A*DLOG(1D0-P) +(B/(BETA*THETA))*DLOG(BTP)
   &    -(C/GAMMA)*(DEXP(-P*GAMMA)-1D0)
      NEWF=GSM*CNT(1)*THETA*LOGS/(EE)
      END
. . . . . . . . . . . . . . . . . . . . . . . . . . . . . .
. . . . . . . . . . . . . . . . . . . . . . . . . . . . . .




. . . . . . . . . . . . . . . . . . . . . . . . . . . . . .
. . . . . . . . . . . . . . . . . . . . . . . . . . . . . .
* Subroutine to calculate the prediction made by Bhadehshia
* for the reaction kinetics of bainite, old theory (1982)
      DOUBLE PRECISION FUNCTION OLDF(P,TC,THETA,FM)
      IMPLICIT DOUBLE PRECISION (A-H,L-Z)
      IMPLICIT INTEGER(I-K)
      DIMENSION CNT(4)
      PARAMETER (R=8.314D0,S=0.69D-03)
      COMMON WS,GSM,CNT(4)
      BBB = 199.999D0
      C3 = 3.769D0
      C2 = 29709.9D0
      C1C=DEXP(9D0)
      WSS=WS+273.15D0
      TK=TC+273.15D0
      BT=1D0+BBB*THETA
      BTP=1D0+BBB*THETA*P
```

```fortran
      B1B=1D0-1D0/BBB
      GNT=3.636D0*WS-2450.0D0
      GAMMA = 11D0*THETA*FM/(R*TK)
      DD=DEXP(GAMMA/BBB)
      A=DEXP(-GAMMA)/(BT)
      CT=1D0 - DD*(B1B +A*(1D0/BBB+THETA))
      CB=B1B*(1D0+THETA -DD)
      C=CT/CB
      B=1D0-A-C
      IF (BTP .LT. 0.0) THEN
          WRITE (6,*) THETA
          PAUSE '1+BBB*THETA*PSI ¡ 1'
      ENDIF
      LOGS=-A*DLOG(1D0-P) +(B/(BBB*THETA))*DLOG(BTP)
     &   -(C/GAMMA)*(DEXP(-P*GAMMA)-1D0)
      EE=DEXP(C2*(WS-TC)/(R*TK*WSS) +(C3/R)*((FM/TK) -(GNT/WSS)) )
      OLDF=C1C*THETA*EE*LOGS
      END
```

. . . .
. . . .

APPENDIX 4

A Model for Acicular Ferrite Transformation Kinetics During Continuous Cooling

```
. . . . . . . . . . . . . . . . . . . . . . . . . . . . . . . . . . . . . .
* This program is written to run on a Sun Workstation
* In its present form it will use the constants determined for
* Harry's bainite kinetics data
. . . . . . . . . . . . . . . . . . . . . . . . . . . . . . . . . . . . . .
      PROGRAM MAIN
      IMPLICIT DOUBLE PRECISION (A-H,L-Z)
      IMPLICIT INTEGER (I-K)
      CHARACTER*71 IFILE
      DIMENSION TC(2000),XT0(2000),FM(2000),X44(2000),
   &  WEIGH(4),CO(8),AT(8),AR(8)
      COMMON WS,GSM,C1,LAM1,C2,LAM2
      MAX=0.0D0
      MSS=0.0
. . . . . . . . . . . . . . . . . . . . . . . . . . . . . . . . . . . . . .
* Open constants file and read
      OPEN (UNIT=1,FILE='theory/geff6/c')
      READ (1,*) C1,LAM1,C2,LAM2
. . . . . . . . . . . . . . . . . . . . . . . . . . . . . . . . . . . . . .
* Read alloy file name and open the file
      READ (5,*) IFILE
      OPEN (UNIT=4,FILE=IFILE)
. . . . . . . . . . . . . . . . . . . . . . . . . . . . . . . . . . . . . .
      OPEN (UNIT=7,FILE='theory/geff6/num')
      OPEN (UNIT=8,FILE='theory/geff6/iweight')
      OPEN (UNIT=9,FILE='temp.dat')
. . . . . . . . . . . . . . . . . . . . . . . . . . . . . . . . . . . . . .
      READ (8,*) IWEIGHT
. . . . . . . . . . . . . . . . . . . . . . . . . . . . . . . . . . . . . .
* Read in the data concerning inclusion content,and composition
      CALL DATAREAD(CO,AR,ALO,MNO)
* Read in thermodynamic data for the alloy considered
      CALL THREAD(WS,BS,MS,XBAR,TC,XT0,FM,X44,J1)
. . . . . . . . . . . . . . . . . . . . . . . . . . . . . . . . . . . . . .
      WEIGH(1)=ALO/121.0D0
      WEIGH(2)=MNO/116.0d0
      WEIGH(3)=((ALO/3.0D0)+MNO)/156.33D0
      WEIGH(4)=1.0d0
. . . . . . . . . . . . . . . . . . . . . . . . . . . . . . . . . . . . . .
* At present the program is set up to vary the nucleation site
* density parameter. The best value from output for all welding
* alloys is the selected for optimim results. For this purpose
* the grain size dependent variable GSM is varied. For the case
* transformation to bainite set GR=1.0, GSM=grain size (microns)
```

* and set IWEIGHT=4.

. . . .
```
        DO  919 GR=1.91,3.0,0.05
            GSM=1.0d0/(WEIGH(IWEIGHT)*GR)
```
. . . .
```
            I3=0
            IC=0
            TOT=0
            TSTEP=0
            MAX=0
            DO  40 I3=1,J1
```
. . . .
* Establishment of the continuous curve as a series of isothermal
* hold
* IF IPROF equals some number other than 0, a linear cooling rate
* employed. The desired cooling rate MUST BE SPECIFIED.

. . . .
```
                IPROF=0
                IF (IPROF .EQ. 0 ) THEN
                    TSTEP=TFUN(TC(I3+1))-TFUN(TC(I3))
                    IF (I3 .EQ. 1) THEN
                        TOT=TFUN(TC(I3))
                    ELSE
                        TOT=TOT+TSTEP
                    ENDIF
                ELSE
                    CR=15.0D0
                    TSTEP=TLFUN(TC(I3+1),CR)-TLFUN(TC(I3),CR)
                    IF (I3 .EQ. 1) THEN
                        TOT=TLFUN(TC(I3),CR)
                    ELSE
                        TOT=TOT+TSTEP
                    ENDIF
                ENDIF
```
. . . .
* Calculation of the volume fraction of ferrite formed at the end
* of the first isothermal hold. Then at subsequent temperatures the
* effective time for formation of the existing amount of ferrite is
* calculated, then growth is allowed for the duration of the current
* isothermal hold.

. . . .
```
                IF ((XT0(I3) .GT. XBAR) .AND. (X44(I3) .GT. XBAR)) THEN
                    IF (TC(I3) .GT. (MS+1.0d0)) THEN
                        IC=IC+1
                        THETA= (XT0(I3)-XBAR)/(XT0(I3)-S)
                        IF (IC .GT. 1) THEN
                            P=V/THETA
                            TIME=NEWF(P,TC(I3),THETA,FM(I3),XBAR)+TSTEP
                        ELSE
```

```
                        TIME=TSTEP
                     ENDIF
                     CALL PROOT(TC(I3),XT0(I3),FM(I3),X44(I3),P,TIME,
      &                 THETA,XBAR)
                     TR=TC(I3)
                     V=P*THETA
                     IF (V .GT. MAX) THEN
                         MAX=P*THETA
                     ENDIF
                  ELSE
                     GOTO 918
                  ENDIF
               ENDIF
40            CONTINUE
918           WRITE (6,928) MAX,GR
928           FORMAT ('  ' 2F13.6,2D15.5)
              ICOUNT=ICOUNT+1
919      CONTINUE
         WRITE (7,*) ICOUNT
17       END




. . . . . . . . . . . . . . . . . . . . . . . . . . . . . . . . . . . .
         DOUBLE PRECISION FUNCTION TFUN(T)
         IMPLICIT DOUBLE PRECISION (A-H,K-Z)

. . . . . . . . . . . . . . . . . . . . . . . . . . . . . . . . . . . .
* Continuous cooling curve expression for arc weld
* (Gretoft, Bhadeshia & Svensson,
* Present parameters are set to submerged are values.

. . . . . . . . . . . . . . . . . . . . . . . . . . . . . . . . . . . .
         CURR=500.0D0
         V=29.0D0
         S=0.92D-02
         EFF=0.95
         TINIT=900.0D0
         TI=200.0D0
         C1=0.4359D+04
         C2=0.151D+01
         TFUN=CURR*V*EFF*((TINIT-TI)**(1.0D0-C2)-
      &  (T-TI)**(1.0D0-C2))/(C1*S*(1.0D0-C2))
         END




         SUBROUTINE PROOT(TC,XT0,FM,X44,P,TIME,THETA,XB)
         IMPLICIT DOUBLE PRECISION (A-H,L-Z)
```

181

```
. . . . . . . . . . . . . . . . . . . . . . . . . . . . . . . . . . . . . . .
* Subroutine to find the normalised volume fraction that satisfies
* the kinetics equation for a given reaction time.
. . . . . . . . . . . . . . . . . . . . . . . . . . . . . . . . . . . . . . .
          IMPLICIT INTEGER (I-K)
          IC=0
          P1=0.1D-08
          P3=0.9999
1         P2=0.5D0*(P1+P3)
          IC=IC+1
          IF (IC .GT. 50) GOTO 11
          IF(DABS(TROOT(P2,TC,THETA,FM,TIME,XB)) .LT. 0.01d0) GOTO 11
          IF (TROOT(P2,TC,THETA,FM,TIME,XB)
     &        *TROOT(P1,TC,THETA,FM,TIME,XB) .LT. 0.00) THEN
             P3=P2
             GOTO 1
          ELSE
             P1=P2
             GOTO 1
          ENDIF
11        P=P2
          END




. . . . . . . . . . . . . . . . . . . . . . . . . . . . . . . . . . . . . . .
          DOUBLE PRECISION FUNCTION NEWF (PSI,TCC,THETA,GM0,XB)
          IMPLICIT DOUBLE PRECISION (A-H,L-Z)
          IMPLICIT INTEGER (I-K)
          COMMON WS,GSM,C1,LAM1,C2,LAM2
          PARAMETER (R=8.314D0,RR=2540D0)
          WSS=WS+273.15D0
          T=TCC+273.15D0
          GNT= 3.636*(T-273.15) -2540D0
          GNW= 3.636*(WSS-273.15) -2540D0
          GAMMA= C2*(GM0-GNT)/(R*RR*T)
          BETA= LAM1*(1.0d0 - LAM2*XB)
          LL =LOGS(PSI,GAMMA,BETA,THETA)
          E = DEXP(-C2/(R*T) -C2*GM0/(RR*R*T))
          NEWF = C1*GSM*THETA*LL/E
          END




. . . . . . . . . . . . . . . . . . . . . . . . . . . . . . . . . . . . . . .
          DOUBLE PRECISION FUNCTION TROOT(PSI,TC,THETA,GM0,TIME,XB)
          IMPLICIT DOUBLE PRECISION (A-H,L-Z)
```

```
          IMPLICIT INTEGER (I-K)
. . . . . . . . . . . . . . . . . . . . . . . . . . . . . . . . . . . . . . . . . . . . . . .
* Function representing the reaction time to form a normalised
* volume fraction PSI at tempreature TC.
. . . . . . . . . . . . . . . . . . . . . . . . . . . . . . . . . . . . . . . . . . . . . . .
          COMMON WS,GSM,C1,LAM1,C2,LAM2
          PARAMETER (R=8.314D0,RR=2540D0)
          T=TC+273.15D0
* WSS=WS+273.15D0
          GNT= 3.636*(T-273.15) -2540D0
* GNW= 3.636*(WSS-273.15) -2540D0
          GAMMA= C2*(GM0-GNT)/(R*RR*T)
          BETA= LAM1*(1.0D0-LAM2*XB)
          LL =LOGS(PSI,GAMMA,BETA,THETA)
          E = DEXP(-C2/(R*T) -C2*GM0/(RR*R*T))
          TROOT=TIME-C1*GSM*THETA*LL/E
          END




. . . . . . . . . . . . . . . . . . . . . . . . . . . . . . . . . . . . . . . . . . . . . . .
          DOUBLE PRECISION FUNCTION LOGS(PSI,GAMMA,BETA,THETA)
          IMPLICIT DOUBLE PRECISION (A-H,L-Z)
          IMPLICIT INTEGER (I-K)
. . . . . . . . . . . . . . . . . . . . . . . . . . . . . . . . . . . . . . . . . . . . . . .
* Function representing the log and exponential terms involving
* PSI in the kinetics equation.
. . . . . . . . . . . . . . . . . . . . . . . . . . . . . . . . . . . . . . . . . . . . . . .
          A=DEXP(-GAMMA)/(1D0+BETA*THETA)
          C=CT(GAMMA,BETA,THETA)/CB(GAMMA,BETA,THETA)
          B= 1D0-A-C
          LOGS=(-A*DLOG(1D0-PSI)
     &     +(B/(BETA*THETA))*DLOG(1D0+BETA*THETA*PSI)
     &     -(C/GAMMA)*(DEXP(-PSI*GAMMA)-1D0))
          END




. . . . . . . . . . . . . . . . . . . . . . . . . . . . . . . . . . . . . . . . . . . . . . .
          SUBROUTINE DATAREAD(COO,ARR,ALOO,MNOO)
          IMPLICIT DOUBLE PRECISION (A-H,L-Z),INTEGER(I-K)
          DIMENSION COO(8),ARR(8)
. . . . . . . . . . . . . . . . . . . . . . . . . . . . . . . . . . . . . . . . . . . . . . .
          READ (5,*) TI,AL,O
. . . . . . . . . . . . . . . . . . . . . . . . . . . . . . . . . . . . . . . . . . . . . . .
* Read the alumina and magnesia content
          READ (5,*) ALOO,MNOO
```

```
. . . . . . . . . . . . . . . . . . . . . . . . . . . . . . . . . . . . . .
          * Read alloy composition form the thermodynamics file
          READ (4,*)
          READ (4,*) (COO(I1I),I1I=1,7)
          COO(8)=1D2-ADD(COO,7)
. . . . . . . . . . . . . . . . . . . . . . . . . . . . . . . . . . . . . .
* Input relative atomic weights
          ARR(1)=12.00
          ARR(2)=28.086
          ARR(3)=54.9
          ARR(4)=58.71
          ARR(5)=95.94
          ARR(6)=51.99
          ARR(7)=14.94
          ARR(8)= 55.847
. . . . . . . . . . . . . . . . . . . . . . . . . . . . . . . . . . . . . .
          END




. . . . . . . . . . . . . . . . . . . . . . . . . . . . . . . . . . . . . .
          SUBROUTINE THREAD(WS,BS,MS,XBAR,T1,X1,F1,X4,J1)
          IMPLICIT DOUBLE PRECISION (A-H,L-Z),INTEGER(I-K)
          DIMENSION TTC(2000),TXT0(2000),TFM(2000),BLAH,TX44(2000)
          DIMENSION T1(2000),X1(2000),F1(2000),X4(2000)
. . . . . . . . . . . . . . . . . . . . . . . . . . . . . . . . . . . . . .
* First two line of data have already been read
* Next line contains start temperatures and the mean carbon
* mole fraction
          READ (4,*) WS,BS,MS,XBAR
. . . . . . . . . . . . . . . . . . . . . . . . . . . . . . . . . . . . . .
* Read thermodynamic quantities:
* Temp, XT0, Driving Force (GM), XAE3 (not used), XN0
          DO 10 I1=1,2000
              READ (4,*,END=11) TTC(I1),TXT0(I1),TFM(I1),BLAH,TX44(I1)
10        CONTINUE
. . . . . . . . . . . . . . . . . . . . . . . . . . . . . . . . . . . . . .
11        J1=I1-1
. . . . . . . . . . . . . . . . . . . . . . . . . . . . . . . . . . . . . .
* Reverse the order so that temperature decreases with array no.
          DO 20 I2=1,J1
              T1(I2)=TTC(I1-I2)
              X1(I2)=TXT0(I1-I2)
              F1(I2)=TFM(I1-I2)
              X4(I2)=TX44(I1-I2)
20        CONTINUE
. . . . . . . . . . . . . . . . . . . . . . . . . . . . . . . . . . . . . .
          END
```

. . . .
* CT is the numerator of the constant C (from separation of
* the differential equation into partial fractions (Bhadeshia
* 1982). CB is the denominator of the same constant.

. . . .

```
        DOUBLE PRECISION FUNCTION CT(GAMMA,BETA,THETA)
        IMPLICIT DOUBLE PRECISION (A-H,L-Z)
        IMPLICIT INTEGER (I-K)
        CT=1D0-DEXP(GAMMA/BETA)*(1D0-(1D0/BETA))
     &    -DEXP((GAMMA/BETA) -GAMMA)
     &    *((1D0/(BETA*(1D0+BETA*THETA)))
     &     + (THETA/(1D0+BETA*THETA)))
        END
        DOUBLE PRECISION FUNCTION CB(GAMMA,BETA,THETA)
        IMPLICIT DOUBLE PRECISION (A-H,L-Z)
        IMPLICIT INTEGER (I-K)
        CB=(1D0-1D0/BETA)*(1D0+THETA-DEXP(GAMMA/BETA))
        END
```

. . . .

. . . .
* Included so that linear cooling curve can be chosen
. . . .

```
        DOUBLE PRECISION FUNCTION TLFUN(CTEMP,CR)
        IMPLICIT DOUBLE PRECISION (A-H,L-Z),INTEGER(I-K)
        TLFUN=(900.0-CTEMP)/CR
        END
```

. . . .

. . . .
* Function to add the elements within an array up to a
* specified number
. . . .

```
        DOUBLE PRECISION FUNCTION ADD(X,I)
        IMPLICIT DOUBLE PRECISION (A-H,L-Z),INTEGER (I-K)
        DIMENSION X(8)
        A=0.
        DO  10 I1=1,I
            A=A+X(I1)
10          CONTINUE
        ADD=A
        END
```

. . . .

APPENDIX 5

A Model for the Hardness of High Strength Weld Microstructures

```
        IMPLICIT DOUBLE PRECISION (A-H,L-Z),INTEGER(I-K)
        INTEGER IARR,IADD,IALL
        PARAMETER (IARR=8,IADD=IARR-1,IALL=1)
        COMMON IAR,IAL
```

. . . .

* IARR=ARRAY SIZE, IALL=NUMBER OF ALLOYS ANALYSED

. . . .

```
        DIMENSION C(IARR,IALL),AT(IARR,IALL),AR(IARR)
        DIMENSION ATP(IARR,IALL),CP(IARR,IALL),HTOT(IALL),V(IALL)
```

. . . .

```
        WRITE (6,*) ' REMEMBER THAT NITROGEN MUST BE IN THE DATASET'
```

. . . .

```
        IAR=IARR
        IAL=IALL
        DO  10 I1=1,IALL
            READ (5,*) (C(J1,I1),J1=1,IADD),V(I1),HTOT(I1)
            C(IARR,I1)=100.0-ADD(C,I1,IADD)
10      CONTINUE
        AR(1)=12.00
        AR(2)=28.086
        AR(3)=54.9
        AR(4)=58.71
        AR(5)=95.94
        AR(6)=51.99
        AR(7)=14.94
        AR(8)=55.847
        MIN=1D10
        K=353.70d0
```

. . . .

* Decides whether to optimise or print out results

. . . .

```
1       K=K+1.0D0
        SUMM=0.0D0
```

. . . .

```
        DO  20 I2=1,IAL
            CALL ATFRAC(C,AT,AR,I2)
            STRSUB=DELSIG(AT,I2)
            STRNIT=NITROG(C,I2)
            STRENGTH=STRSUB+STRNIT
            CALL ENRICH(V,AT,ATP,I2)
            CALL WT(ATP,CP,AR,I2)
            STRM=3.0D0*MNH(C,I2)
```

. . . .

* Variable Separation for Phoenix analysis

. . . .

```fortran
          YY= 3.0D0*HTOT(I2) - STRM*(1.0D0-V(I2)) -
     &         V(I2)*STRENGTH
          XX=V(I2)

*  .  .  .  .  .  .  .  .  .  .  .  .  .  .  .  .  .  .  .  .  .  .

          PRED= V(I2)*(STRENGTH+K) +(1.0D0-V(I2))*STRM
          SUMM = SUMM+ (PRED-3.0D0*HTOT(I2))**2.0
          WRITE (6,*) PRED/3d0, HTOT(I2)
*         WRITE (6,*) XX,YY
20        CONTINUE
          IF (SUMM .LT. MIN) THEN
             BEST=K
             MIN=SUMM
          ENDIF
          ICOUNT=ICOUNT+1
*         IF (ICOUNT .LT. 1000) GOTO 1
          END
```

. . . .

* General function to add elements in an array

. . . .

```fortran
          DOUBLE PRECISION FUNCTION ADD(X,I,IX)
          IMPLICIT DOUBLE PRECISION (A-H,L-Z),INTEGER (I-K)
          COMMON IARR,IALL
          DIMENSION X(IARR,IALL)
          A=0.
          DO  10 I1=1,IX
             A=A+X(I1,I)
10        CONTINUE
          ADD=A
          END
```

. . . .

* Subroutine to convert weight percentages into atomic fractions

. . . .

```fortran
          ATFRAC(CC,CAT,ARR,IAT)
          IMPLICIT DOUBLE PRECISION (A-H,L-Z),INTEGER(I-K)
          COMMON IARR,IALL
          PARAMETER (IAR=8,IAL=10)
          DIMENSION CC(IARR,IALL),COM(IAR,IAL),CAT(IARR,IALL)
          DIMENSION SUM(IAL),ARR(IARR)
          DO  10 J1=1,IARR
             COM(J1,IAT) = CC(J1,IAT)/ARR(J1)
10        CONTINUE
          SUM(IAT)=ADD(COM,IAT,IARR)
          DO  13 J2=1,IARR
             CAT(J2,IAT)=COM(J2,IAT)/SUM(IAT)
13        CONTINUE
          END
```

. . . .

* Calculates the strengthening contributions
* of substitutional elements in iron

. . . .

```
        DOUBLE PRECISION FUNCTION DELSIG(AT1,JD)
        IMPLICIT DOUBLE PRECISION (A-H,L-Z),INTEGER(I-K)
        COMMON IARR,IALL
        DIMENSION AT1(IARR,IALL)
        SFE=220.
        STOT= SFE + AT1(2,JD)*(5215.0D0)
     &  + AT1(3,JD)*3510.33D0
     &  + AT1(4,JD)*3937.667D0
     &  + AT1(6,JD)*93.967D0
        DELSIG=STOT
        END
```

. . . .

. . . .

* Calculates the effect of carbon enrichment on austenite composition
* atomic fractions

. . . .

```
        ENRICH (VE,ATE,APE,IE)
        IMPLICIT DOUBLE PRECISION (A-H,L-Z),INTEGER (I-K)
        COMMON IARR,IALL
        PARAMETER (IAR=8,IAL=10)
        DIMENSION ATE(IARR,IALL),APE(IAR,IAL)
        PARAMETER (S=0.69D-03)
        XGP = (ATE(1,IE) - VE*S)/(1.0D0-VE)
        APE(1,IE)=XGP
        DO  10 I1=2,8
            APE(I1,IE)=ATE(I1,IE)*(1.0D0-XGP)
10      CONTINUE
        END
```

. . . .

* Calculates the weight percentage from atomic fractions

. . . .

```
        WT(AW,CW,ARW,IW)
        IMPLICIT DOUBLE PRECISION (A-H,L-Z),INTEGER (I-K)
        COMMON IARR,IALL
        DIMENSION CW(IARR,IALL),AW(IARR,IALL),ARW(IARR,IALL)
        TOT=0.0
        DO  10 I1=1,IARR
            TOT=TOT + AW(I1,IW)*ARW(I1,IW)
10      CONTINUE
        DO  11 I2=1,IARR
            CW(I2,IW)=1.0D+02*(AW(I2,IW)*ARW(I2,IW)/TOT)
11      CONTINUE
        END
```

. . . .

* Calculated the hardness of martensite for a given composition

. . . .

```
        DOUBLE PRECISION FUNCTION MNH(CM,IM)
        IMPLICIT DOUBLE PRECISION (A-H,L-Z),INTEGER(I-K)
        COMMON IARR,IALL
        DIMENSION CM(IARR,IALL),CF(6)
        CF(1)= 670.0D0
        CF(2)= -73.0D0
        CF(3)= 34.0D0
        CF(4)=12.0D0
        CF(5)=-8.0D0
        CF(6)=61.0D0
        MNH= CF(1)*DSQRT(CM(1,IM))
    &   +CF(2)*CM(2,IM)
    &   +CF(3)*CM(3,IM)
    &   +CF(4)*CM(4,IM)
    &   +CF(5)*CM(5,IM)
    &   +CF(6)*CM(6,IM) +132.0d0
        END
```

. . . .

* Calculates the effect of nitrogen on strength

. . . .

```
        DOUBLE PRECISION FUNCTION NITROG(CC,INIT)
        IMPLICIT DOUBLE PRECISION (A-H,L-Z),INTEGER(I-K)
        COMMON IARR,IALL
        DIMENSION CC(IARR,IALL)
        NIT=CC(7,INIT)
        NITROG=7.35D0 - 4400D0*NIT - 59400D0*(NIT**2)
        END
```

REFERENCES

AARONSON H.I.
The Decomposition of Ausenite by Diffusional Processes Zackay V.F. & Aaronson H.I. eds. Interscience NY pp. 387-545, 1962.

AARONSON H.I., HALL M.G., BARNETT D.M. & KINSMAN K.R.
Scripta Metall. **9** p. 705, 1975.

ALI A. and BHADESHIA H.K.D.H.
Materials Science and Technology **5** pp. 398–402, 1989.

ALI A. and BHADESHIA H.K.D.H.
Materials Science and Technology **6** pp. 781-784, 1990.

ANDERSON J.C., LEAVER K.D., RAWLINGS R.D. & ALEXANDER J.M.
Materials Science, 3rd ed. Van Nostrand Reinhold, Workingham, England p. 268, 1985.

BARRITE G.S.
Ph.D. Thesis 1982.

BHADESHIA H.K.D.H.
Sripta Metall. **14** p. 821, 1980.

BHADESHIA H.K.D.H.
Acta. Metall. **29** pp. 1117-1130, 1981a.

BHADESHIA H.K.D.H.
Metal Sci. **15** p. 174, 1981b.

BHADESHIA H.K.D.H.
Metal Sci. **15** p. 178, 1981c.

BHADESHIA H.K.D.H.
Metal Sci. **16** pp. 156-165, 1982a.

BHADESHIA H.K.D.H.
J. de Physique **43** C4 pp. 443–448, 1982b.

BHADESHIA H.K.D.H.
Phase Transformations in Ferrous Alloys, editors A. R. Marder and J. I. Goldstein, TMS–AIME, Warrandale, Pennsylvania, USA **pp. 335–340,** 1984.

BHADESHIA H.K.D.H.
Progress in Materials Science **29** pp. 321-386, 1985.

BHADESHIA H.K.D.H.
Mat. Sci. & Tech. **1** pp. 497-504, 1985.

BHADESHIA H.K.D.H.
Proceedings of an International Conference: Phase Transformations '87,ed. G. W. Lorimer, Institute of Metals, London, pp. 309-314, 1988.

BHADESHIA H.K.D.H
Steel Technology International, Sterling Publications, London,   pp. 289–294, 1989.

BHADESHIA H.K.D.H. & CHRISTIAN J.W.
Metall. Trans. A **21A** pp. 767-797, 1990.

BHADESHIA H.K.D.H. and EDMONDS D.V.
Metall. Trans. A **10A** pp. 895–907, 1979.

BHADESHIA H.K.D.H. & EDMONDS D. V.
Acta. Metall. **28** pp. 1265-1273, 1980.

BHADESHIA H.K.D.H. & SVENSSON L.-E.
Joining and Materials **2** pp. 182R-187R, 1989.

BHADESHIA H.K.D.H. & SVENSSON L.-E.
Joining and Materials **2** pp. 236R-238R, 1989

BHADESHIA H.K.D.H. & SVENSSON L.-E.
J. Mat. Sci. **24** pp. 3180-3188, 1989.

BHADESHIA H.K.D.H., SVENSSON L.-E., & GRETOFT B.
Acta Metall. **33** pp. 1271-1283, 1985.

BHADESHIA H.K.D.H., SVENSSON L.-E., & GRETOFT B.
J. Mat. Sci. **21** pp. 3947-3951, 1986a.

BHADESHIA H.K.D.H., SVENSSON L.-E., & GRETOFT B.
Scand. J. Metall. **15** pp. 97-103, 1986b.

BHADESHIA H.K.D.H., SVENSSON L.-E., & GRETOFT B.
Advances in Welding Technology and Science, ASM, Metals Park, Ohio, U. S. A., pp. 225-229, 1987a.

BHADESHIA H.K.D.H., SVENSSON L.-E., & GRETOFT B.
Proceedings of the Third International Conference on Welding and Performance of Pipelines, published by the Welding Institute, Abington, U.K.   1987b.

BHADESHIA H.K.D.H., SVENSSON L.-E., & GRETOFT B.
Proc, Int. Conf. on Welding Metallurgy of Structural Steels, The Metallurgical Society of the AIME, Warrendale, Pennsylvania. Edited by J. Y. Koo, pp. 517-530, 1987c.

BHADESHIA H.K.D.H. & WAUGH A. R.
Proceedings of the International Solid-Solid Phase Transformations Conference, Pittsburgh, The Metallurgical Society of the A. I. M. E., Warrendale, PA, USA. pp. 993-998, 1981.

CALVO F.A., BENTLEY K.P. & BAKER R.G.
Studies of the Welding Metallurgy of Steels, BWRA, Abington, Cambridge 1963.

CHRISTIAN J.W.
Theory of Transformations in Metals and Alloys, Part I, 2nd edition, Pergamon Press, Oxford, UK. 1975.

CHRISTIAN J.W. and EDMONDS D.V.
Phase Transformations in Ferrous Alloys, eds. A. R. Marder and J. I. Goldstein, TMS–AIME, Warrandale, Pennsylvania, USA pp. 293–327, 1984.

COATES D.E.
Metall. Trans. A **4A** p. 1077, 1973.

COHEN M.
Material Transactions JIM, October 1991.

DADIAN M.
Advances in the Science & Technology of Welding, ed. S.A. David, Metals Park OH. pp. 101-117, 1986.

DAVIES G.J. & GARLAND J.G.
Int. Metall. Rev. **20** pp. 83-106, 1975.

DEB P., CHALLENGER K.D. & THERREIN A.E.
Metall. Trans. A **18A** pp. 987-999, 1987.

DEHOFF R.T. and RHINES F.N. eds.
Quantitative Microscopy, McGraw–Hill Book Company, New York, USA.   1968.

DOWLING J.M., CORBETT J.M. & KERR H.W.
Metall. Trans. A **17A** pp. 1611-23, 1986

EDMONDS D.V and COCHRANE R. C.
Metall. Trans. A **21A** pp. 1527–1540, 1990.

EASTERLING K.E.
Introduction to the Physical metallurgy of Welding Butterworths, London. 1983.

FARRAR R.A. & HARRISON P.L.
J. Mat. Sci. **22** pp. 3812-3820, 1987.

FLECK N.A., GRONG O. & MATLOCK D.K.
Welding Research Supplement to the Welding Journal **pp. 113s-121s,** 1986.

FOWLER R.H. & GUGGENHIEM E.A.
Statistical Thermodynamics Camb. Univ. Press, New York 1939.

FREDRICKSSON H.
Scand. J. Metall. **5** pp. 27-32, 1976.

FREDRICKSSON H.
Acta Ouluensis Series C 26 Proc 3rd Scandinavian Symposim on Materials Science, University of Oulu, Finland. -25 1983.

FROST R.H., MUTH T.R., VAUGHAN T.R. & JORGASON R.R.
Proc. Conf. on 'Metallogrphy and Interpretation of Weld Microstrucures' ASM International, Metals Park, Ohio, USA, pp. 261-277, 1987.

GREGG J.M.
Unpublished research, University of Cambridge. 1992.

GOODENOW R.H., MATAS S.J. & HEHEMANN R.F.
Trans AIMME **227** pp. 651-658, 1963.

GRONG O. & MATLOCK D.K.
Int. Met. Rev. **31** pp. 27-48, 1986.

GRETOFT B., BHADESHIA H.K.D.H. & SVENSSON L.-E.
Acta Stereol. **5** pp. 365-371, 1986.

HAWKINS M.J. & BRADFORD J.
J.I.S.I. **210** pp. 97-105, 1972.

HEHEMANN R.F.
Phase Transformations, ASM, Metals Park, Ohio, USA   pp. 397–432, 1970.

HEHEMANN R.F., KINSMAN K.R., AARONSON H.I.
Metall. Trans. A **3A**   1972.

HILLERT M.
Acta Metall. **1** p. 764, 1953.

ITO Y. & NAKANISHI M.
Sumitomo Search **15** pp. 42-62, 1976.

ITO Y. & NAKANISHI M.
Metal Constr. **14** (9) pp. 472-478, 1982.

KHAN S.A. and BHADESHIA H.K.D.H.
Metall. Trans. A **21A** pp. 859–875, 1990.

KO T. & COTTERLL S.A.
J.I.S.I. **172** pp. 307-312, 1952.

KINSMAN K.R., EICHEN E. & AARONSON H.I.
Metall. Trans. A **6** 303 1975

KLUKEN A.O., GRONG O.
Metall. Trans. A **20 A** pp. 1335-1349, 1989.

LACHER J.R.
Proc. Camb. phil. Soc. math. phys. Sci. **33** p. 518, 1937.

LANCASTER W.F.
Metallurgy of Welding, Brazing and Soldering 2nd ed. George Allen & Unwin 1970.

MAGEE C.L.
Phase Transformations, ASM, Metals Park, Ohio, USA pp. 115–156 1970.

MAYNIER P.H., JUNGMANN B. & DOLLET J.
Hardenability Concepts with Applications to Steel, eds. D.V. Doane & J.S. Kirkaldy The Metall. Soc. of AIME pp 518-544, 1978.

MILLS A.R., THEWLIS G. & WHITEMAN J.A.
Mater. Sci. & Thechnol. **3A** pp. 1051-61, 1987.

OHMORI Y., OHTANI H. and KUNITAKE T.
Trans. I.S.I.J. **11** 250–259, 1971.

OLSON G.B. & COHEN M.
Metall. Trans. A **7A** pp. 1915-1923, 1976.

PICKERING F.B.
Proceedings of an International Conference on Electron Microscopy, Springer Verlag OHG, Berlin, Germany pp. 628–637, 1958.

RAO M.M. and WINCHELL P.G.
Trans. AIME **239** pp. 956–960, 1967.

RICKS R.A.,HOWELL P.R. & BARRITE G.S.
J. Mat. Sci. **17** pp. 732-740, 1982.

RUSSELL K.C.
Acta Metall. **16** p. 761, 1968.

RUSSELL K.C.
Acta Metall. **17** p. 1123, 1969.

SPEICH G.R. & COHEN M.
Trans. TMS-AIME **218** pp. 1050-1059, 1960.

SPEICH G.R. & WARLIMONT H.
J.I.S.I. **206** pp. 385-392, 1968.

STRANGWOOD M.
Ph.D. Thesis University of Cambridge 1986.

STRANGWOOD M. & BHADESHIA H.K.D.H.
Advances in Welding Technology and Science ASM, Metals Park, Ohio, U. S. A pp. 209-213, 1987.

STRANGWOOD M. & BHADESHIA H.K.D.H.
Phase Transformations '87 ed. G.W. Lorimer, Institute of Metals, London pp. 466-470, 1988.

SUGDEN A.A.B. & BHADESHIA H.K.D.H.
Metall. Trans. A **19A** pp. 669-674, 1988a.

SUGDEN A.A.B. & BHADESHIA H.K.D.H.
Metall. Trans. A **19A** pp. 1597-1602, 1988a.

SUGDEN A.A.B. & BHADESHIA H.K.D.H.
Metall. Trans. A **20A** pp. 1811-1818, 1989.

SUGDEN A.A.B. & BHADESHIA H.K.D.H.
Recent Trends in Welding Science and Technology (TWR '89), eds. S.A. David and J.M. Vitek ASM International, Ohio, U. S. A., pp. 745-748, 1989a.

STEVEN W.G. & HAYNES A.G.
J.I.S.I **183** p. 349, 1956.

SVENSSON L.-E.
Private Communication, 1988.

SVENSSON L.-E. & BHADESHIA H.K.D.H.
Proceedings of an International Conference on Improved Weldment Control using Computer Technology, Vienna, Austria, Pergamon Press, Oxford, pp. 71-78, 1988.

SVENSSON L.-E., GRETOFT B. & BHADESHIA H.K.D.H.
Proceedings of an International Conference on Computer Technology in Welding, published by The Welding Institute, Abington, U.K. 1986.

TAKAHASHI M & BHADESHIA H.K.D.H.
Mat. Sci. & Tech. **6** pp. 592-603, 1990.

TRIVEDI R. & POUND G.M.
J. Appl. Phys. **40** pp. 4293-4300, 1969.

TWEED J.H. & KNOTT J.F.
Acta Metall. **35** pp. 1401-1414, 1987.

WATSON J.D. & McDOUGALL
Acta Metall. **21** pp. 961-973, 1973.

YANG J.R. & BHADESHIA H.K.D.B.
Advances in Welding Technology and Science ASM, Metals Park, Ohio, U. S. A. pp. 187-191, 1987.

HSU T.Y. & MOU YIWEN
Proceedings of an International Conference on Phase Transformations in Ferrous Alloys, Philadelphia A.I.M.E., pp. 335-340, 1983.